Assessment of Soft X-Rays for Detection of Fungal Infection in Stored Wheat

by

Dipali Shridhar Narvankar

A Thesis submitted to the Faculty of Graduate Studies of

The University of Manitoba

in partial fulfilment of the requirements of the degree of

MASTER OF SCIENCE

Department of Biosystems Engineering

University of Manitoba

Winnipeg, Manitoba

THE UNIVERSITY OF MANITOBA

FACULTY OF GRADUATE STUDIES

*****

COPYRIGHT PERMISSION

Assessment of Soft X-Rays for Detection of Fungal Infection in Stored Wheat

BY

Dipali Shridhar Narvankar

A Thesis/Practicum submitted to the Faculty of Graduate Studies of The University of Manitoba in partial fulfillment of the requirement of the degree

Of

Master of Science

ABSTRACT

Fungal infection is responsible for 5 to 10% of global food losses which can be reduced by early detection of fungal infection. Conventional methods currently being used for fungal detection are time consuming and tedious. Therefore, a fast, reliable, user friendly and easily upgradeable fungal detection method is necessary. In this study, the potential of a soft X-ray method for detection of fungal infection in stored wheat was explored. X-ray images of healthy wheat kernels and wheat kernels infected with *Aspergillus niger*, *Aspergillus glaucus*, and *Penicillium* spp. were acquired at 184 μA current and 13.6 kV voltage. A total of 34 features extracted from X-ray images were used to discriminate healthy and fungal-infected kernels. Statistical classifiers (linear, quadratic, and Mahalanobis) were applied to develop two-class, and four-class models. The maximum classification accuracy of 98.9% was obtained by the two-class model. The Mahalanobis discriminant classifier correctly identified on average 94.4% infected kernels. Four-class linear and quadratic classifiers could identify *Penicillium* with accuracy greater than 85%. Conversely, *A. niger*, *A. glaucus*, and healthy kernels were poorly classified by all statistical classifiers.

ACKNOWLEDGEMENT

"No one walks alone and when one is walking on the journey of life just where do you start to thank those that joined you, walked beside you, and helped you along the way?" (Hooker, 2007).

First of all, I humbly bow my head before the God to whom I owe my existence.

I am highly obliged to my advisor Dr. Digvir Jayas, Department of Biosystems Engineering for giving me the golden opportunity to study at the University of Manitoba, Canada. His enthusiastic and positive nature always inspired me to work steadily. His guidance was very precious to drive my research work in the right direction.

I am very grateful to my committee members, Dr. White and Dr. Fazel for their valuable suggestions, continuous help, and encouragement throughout the courses and research work. Their comments helped me to improve my thesis work. I am also grateful to all course teachers who helped me a lot to acquire knowledge and move towards my aim.

I really appreciate the staff of the Department of Biosystems Engineering and International Centre for Students for the cooperation and moral support.

This work would be incomplete without special mention of Girija didi, Dr. Bhatakar, Ashokmama, Vilasbhau, and Sunilmama who helped me to complete my dream of

higher education in a foreign country. I would be always thankful for their financial support, understanding, and the love for education.

I am really thankful for cheerful and encouraging company of Ashwini Borkar, Asit Dey, Prachi Rajguru, Abhishek Gupta, Nishant Dhruve, Anju Bajaj, Sharmili Sarkar, and Parnali Chowdhury. They helped me to overcome the worries and to be strong minded.

I am indebted to my colleagues Chandra Singh, Rupalal Chawdhary, Prabal Ghosh, Chelladurai Vellaichamy, Mahesh Sivakumar, Raja Ramachandran, Suresh Neethirajan, Gayathri Pichai, Vadivambal Rajagopal, and Nithya Udaykumar for their guidance and maintaining healthy atmosphere for work.

There are no words to express my gratitude towards my parents, Dada, Vahini, Didi, and Jiju for their understanding and whole hearted cooperation. With the sense of deep gratification, I cherish the warm wishes, constant inspiration and love of my husband Sagar and my in-laws.

I thank the Canada Research Chairs program and the Natural Sciences and Engineering Research Council of Canada for funding this study. Finally, I like to thank all the people who helped me to complete my study and research work successfully.

TABLE OF CONTENTS

LIST OF FIGURES

LIST OF TABLES

1. INTRODUCTION

The most important cereal crop in Canada is wheat. Canada is the sixth largest wheat producer in the world (Dakers and Frechette, 1998). Total annual production of the wheat in the world is 603 Mt, of which Canada produces 20.1 Mt (USDA, 2008). Most of the wheat production in Canada is concentrated in Ontario and Prairie Provinces (Alberta, Manitoba, and Saskatchewan). Canadian wheat is grouped into eight classes namely Canada Prairie Spring Red (CPSR), Canada Prairie Spring White (CPSW), Canada Western Amber Durum (CWAD), Canada Western Extra Strong (CWES), Canada Western Hard White Spring (CWHWS), Canada Western Red Spring (CWRS), Canada Western Red Winter (CWRW), and Canada Western Soft White Spring (CWSWS). The CWRS class is the largest wheat class in production, area under coverage, and consumer demand.

Canada occupies the second place in wheat exportation in the world preceded by the United States (U.S.) (Dakers and Frechette, 1998). The wheat from Canada is exported mainly to Asia, South America, the Middle East, and the U. S. The grains are inspected for varietal purity, test weight, soundness, vitreousness, foreign material, and insect and fungal infection before shipment. The fungal growth in stored cereals is a serious problem which leads to qualitative and quantitative losses. Fungi are responsible for 5 to 10% of global food losses (Williams and Wood, 1986). Fungal growth causes loss in germinability, discolouration of grain, heating, mustiness, biochemical changes, undesirable odour and appearance, and weight loss of the grain kernels which lowers the grading quality and hence, market value of the crop (Christensen and Meronuck, 1988).

The fungi can be classified into field fungi and storage fungi. Field fungi invade developing and mature seeds in the field before the harvest. This invasion may be severe in a rainy season and in a humid region. The storage fungi mainly attack the grain after harvest except infection of developing ears of corn by *Aspergillus flavus* (Seitz et al., 1975). *Alternaria, Cladosporium, Fusarium*, and *Drechslera* are common species of field fungi while *Aspergillus, Penicillium, Rhizopus*, *Mucor,* and *Nigrospora* are species of storage fungi. If grains are heavily infected by field fungi then they become more resistant to storage fungi (Seitz et al., 1975). Some fungi may have a few beneficial uses, e.g., *A. niger* can be used in preparing artificial citric acid and *A. flavus* is used to produce a sweetened rice juice called Koji (Grainaissance Inc., 1999).

The main threat for stored cereals arise from *Aspergillius* spp., *Penicillium* spp., and the field fungus *Fusarium* spp. which may produce mycotoxins such as aflatoxin, cithrinin, xanthoquinones, ochratoxin A, Sterigmatocystin, and Penicillic acid. Though visual molds can be removed from the kernels, mycotoxins can not be removed from the final products as they are usually integral to grain kernels and are not degraded during processing. Therefore, final products can be poisonous for the consumer. Also, utilization of the raw material by removing infected parts can be dangerous since toxins can be spread to uninfected parts by diffusion (Gourama and Bullerman, 1995). Fungi reproduce through the production of spores which are generally microscopic and invisible to the naked eye. Therefore, the first stage of development of fungi cannot be detected without a microscope. Wind, insects, birds, and contaminated trucks and equipment aid in the dispersal of the spores which

remain dormant until the proper conditions for growth occur. Generally, the fungi need 70% relative humidity and temperature over 30°C for several days to a week to start their life cycle (Council for Agricultural Science and Technology, 1989). The suitable conditions for growth are specific for each particular group of fungi and therefore, growth of particular fungi may be stopped by changing the surrounding conditions, i.e., temperature and humidity but those changes may lead to the growth of different fungi. In grains, adequate food supply, environmental conditions, and exposure duration affect the extent of fungal contamination. Also, exposure of under-dried grains to the changes in weather may provide proper conditions for fungi to continue their growth. In severe cases, fungal infection can be responsible for the death of animals and human beings. International Agency for Research on Cancer (IARC) (Council for Agricultural Science and Technology, 1989) stated that there is definite link between Aflatoxin B_1 and cancer in animals. Mycotoxins have probable links with birth defects in animals, nervous system problems, and tumours of liver, kidneys, digestive tract, urinary tract, and the lungs (Council for Agricultural Science and Technology, 1989).

Proper control measures in combination with an efficient detection technique may help in controlling storage losses which occur due to fungal infection. Chemical methods, immunological method, electrical impedance method, selective and differential media, fungal volatiles, most probable number (MPN) method, Howard mold count (HMC) method, polymerase chain reaction (PCR), and image analysis method are currently being used to detect fungal infections (Sukurai and Shiota, 1977; Seitz et al., 1977, 1979; Brodsky et al., 1982; Jarvis et al., 1983; Gaunt et al., 1985; Notermans et al., 1986; Sashidhar et al., 1988; Kamphuis et al., 1989; Notermans and

Kamphuis, 1992; Borjesson et al., 1993; Zeringue et al., 1993; Gourama and Bullerman, 1995; Manonmani et al., 2005; Scotter et al., 2005; Pearson and Wicklow, 2006; Singh et al., 2007). These methods are reliable but most of these methods are time consuming and tedious since sample preparation requires a long time. The proteins and carbohydrates of the cereals may interfere with the fungi which may lead to misinterpretation of the results. Also, these methods need skilled personnel. Therefore, it is necessary to develop an ideal method for the detection of fungal infection which will be fast, reliable, user friendly, and easily upgradable.

As compared to conventional methods, soft X-ray method is a simple, fast, and non destructive method. The reviewed literature revealed that the soft X-ray method could be used for detection of internal defects and insect infection in agricultural produce (Karunakaran et al., 2004a, 2004b; Neethirajan et al., 2004). Sprouting and vitreousnss can also be detected successfully by this method (Neethirajan et al., 2007a, 2007b). The soft X-ray method has also shown potential in the fungal detection (Pearson and Wicklow, 2006). Fungal infection in grains leads to change in the density of the grains. This density change can be detected by comparing the features extracted from the X-ray images of healthy and infected kernels. Statistical classifiers and artificial neural network (ANN) based on pattern recognition techniques can be used for detection of fungal infection (Jayas et al., 2000; Karunakaran et al., 2004a, 2004b; Neethirajan et al., 2004; Neethirajan et al., 2007a, 2007b). Therefore, this study was undertaken with the following objectives:

1. To explore the potential of a soft X-ray method to detect fungal infection in wheat by *Aspergillus glaucus*, *A. niger,* and *Penicillium* spp.

2. To extract X-ray image features for development of classification algorithm.

3. To assess the performance of statistical classifiers and ANN in identifying wheat kernels infected by different types of fungi.

2. REVIEW OF LITERATURE

2.1 Background

Several species of fungi produce pathogenic byproducts called mycotoxins and hence, on the basis of this ability, the fungi can be classified into mycotoxic fungi and non-mycotoxic fungi. There is no direct relationship between visible mold in grain and the presence or lack of mycotoxins. Aflatoxin, deoxynivalenol (DON), zearalenone (ZEN), fumonisin, and T-2 are common mycotoxins (Prescott et al., 2007). *Aspergillus, Penicillium, Fusarium, Alternaria*, and *Claviceps* have mycotoxigenic strains of fungi. Mycotoxic molds lower the nutritional quality of grain by decreasing the fat, protein, and vitamin content of the grain and these molds may be toxic to animals and humans. *Alternia, Fusarium*, and *Helminthosporium* species cause seed sterility, germ death, discolouration, and odour in kernels of wheat and barley and typically occur in the field.

Fifty species of *Aspergillus* produce mycotoxins which include aflatoxin, ochratoxin A, sterigmatocystin, cyclopiazonic acid, citrinin, patulin, and tremorgenic toxins. In 1965, the Food and Drug Administration in the USA set the maximum level of Aflatoxin at 20 ppb in all food and feeds (Council for Agricultural Science and Technology, 1989). The *Penicillium* genus includes 150 species out of which 17 species secrete mycotoxins such as citreoviridin, citrinin, cyclopiazonic acid, ochratoxin A., patulin, penitrem A, PR toxin, Roquefortine C, and Secalonic acid D. These toxins are mainly classified into two groups: toxins affecting liver and kidney functions; and neurotoxins.

Fusarium, a plant pathogen, is mostly found in soil. It can contaminate corn, wheat, barley, rye, triticale, millet, oats, and their products and produce a metabolite called deoxynivalenol (DON) or vomitoxin. *Fusarium graminiarum* can produce deoxyvalenol, zearalenone, 3-acetyldeoxynivalenol, 15-acetylaldeoxynivalenol, diacetyldeoxynivalenol, and diacetoxyscirpenol. *Alternaria* infects plants in fields and may affect wheat, barley, and sorghum by producing toxins which include alternariol, alternariol monomethyl ether, altenuene, tenuzonic acid, and alertoxins.

Many species of fungi may cause diseases in grain and animals. *Claviceps purpurea*, ergot mold, causes human mycotoxicosis which is called ergotism. It can also contaminate barley, oat, rye, and wheat by producing ergotamine. *Penicillium spp.* cause blue green discoloration in the germ area which is called blue eye rot while *Ustilage maydis* is responsible for corn smut. Karnal Bunt (*Tilletia indica*) is a non-mycotoxigenic fungus which is named after Karnal, India. Its spores attack developing kernels within the seed head. There is little or no external sign of infection. The kernels are shrunken at the germ end and covered with the sori which discolor the flour. The kernels then impart a fishy odor. Black tip (black point) is another non-mycotoxigenic fungus associated with seedling blight and root rot which forms dark brown to black sooty mold and hence its name. *Tilletia tritici* and *Tilletia leaves* cause common smut or bunt mainly in winter wheat but sometimes spring wheat is also affected. It reduces wheat yield and grain quality. Infected kernels have a pungent and fishy odor with dark appearance (Wiese, 1991). Direct and indirect losses in grain due to the fungi can be prevented by detecting the fungal infection at very early stages.

2.2 Detection of Fungal Infection

Different fungal detection methods currently being used and their advantages and limitations are discussed in this section.

2.2.1 Fungal enzymes

Fungal species produce a variety of enzymes during deterioration of the grains such as cellulase, polygalacturonase, pectin methyl esterase, 1-4-fl-glucanase, fl-glucosidase, and fl-xylosidase (Sellars et al., 1976) which can be used as an indicator of fungal growth. The enzymes and their production in culture and on mold can be calculated by using chromogenic 4-nitrophenyl substrates (Jain et al., 1991). In this method, 4-nitrophenyl is liberated within 1 h after termination of a reaction which causes an increase in optical density and aids in the measurement of enzyme activity. This method requires 1 to 2 h for fungal detection. The micro-titre plates and a multi-scan plate reader system not only allow analyses of a large number of samples in less time but also can accurately enumerate enzyme activity. The only disadvantage of this method is that it can be used as a rapid method only for selected species in specific conditions because these enzymes may differ in quantity with species of fungi, e.g., *A. flavus* has an ability to produce a large quantity of α-amylase and sucrase as compared to *A. restrictus and Penicillium spp.* (Ghosh and Nandi, 1986, Matrai et al., 2000). Also, enzyme production depends on water activity and temperature of the incubation (Flannigan and Bana, 1980). Therefore, this method hardly provides an overall solution for detection of fungi.

2.2.2 Chemical methods

Fungal infection causes chemical changes in grains which lead to changes in seed color and appearance. Many molds use grain lipids for their growth. The lipids are broken down into free fatty acids and glycerol by lipases. Thus, in a reverse way, one can say that the level of free fatty acid in the grain can be used as indication of mold infection. Chemical methods include determination of chitin, adenosine triphosphate, and ergosterol.

2.2.2.1 Chitin

Chitin is present in the walls of fungal spores and mycelia and it can be detected by using nuceller epidermis of developing wheat kernel as a true biological receptor (Baldo et al., 1982). Fluorescein-labeled wheat germ lectin has a specific binding affinity for N-acetyl-D-glucosamine, which reacts with the nuceller epidermis of a developing wheat kernel and results in fluorescence. This reaction can be completely inhibited if the chitin-like structure is present in the nuceller epidermis wall. This fact was used to indicate the presence of fungi in grain. The concentration of fungi is highly correlated with the glucosamine level (Lin and Cousin, 1985) which can be measured by analyzing chitin $(C_8H_{13}O_5N)n$ (Ride and Drysdale, 1972). Chitin is hydrolyzed to N-acetyl-D-glucosamine and finally deaminated to aldehydes which are measured by a colorimetric method for the presence of fungi in food. N-acetyl-D-Glucosamine content changes with the age and species of fungi (Sukurai and Shiota, 1977).

2.2.2.2 Adenosine triphosphate

Adenosine triphosphate (ATP) is a measure of metabolic activities and the principle of this method is based on the production of light due to the utilization of ATP in the luciferin-luciferase enzyme system. This technique can be used for detection of *Trichoderma reesei* (Gaunt et al., 1985).

2.2.2.3 Ergosterol

Ergosterol is a better tool of detection than plating because ergosterol can detect both viable and non-viable strains of fungi. Ergosterol is a component of fungal cell membranes and the principal sterol of fungi with few exceptions such as certain phycomycetes and rust fungi (Weete, 1980). It serves the same function that cholesterol serves in animal cells. The normal range of ergosterol is 0.2 to 0.6% of the dry weight but it can vary with age and growing conditions (Newell, 1992). Its presence in fungal cells and absence in animal cells make it useful in the preparation of antifungal drugs. High performance liquid chromatography (HPLC) assay was efficient for detection of ergosterol and had a good resolution. At the same time, ergosterol can strongly absorb wavelengths ranging from 240 to 300 nm and hence ultraviolet (UV) light can be used to detect fungi in grain (Seitz et al., 1977, 1979). Sashidhar et al. (1988) iodinated ergosterol to make it fluorescent under long wavelengths of light and then used it as an index of fungal contamination of grains.

2.2.3 Selective and differential media

Selective media inhibits the growth of fungal species other than the one being sought, usually using a combination of antifungal compounds, e.g., *A. flavus* and *A. parasiticus* agar (AFPA) (Pitt et al., 1983, 1990). Conversely, differential media are

used to show an obvious change in the presence of a certain fungal species, e.g., *Apergillus* differential medium (ADM) contains ferric citrate (0.05%) which on reaction with Kojic acid, byproduct of *A. flavus*, produces a bright yellow-orange pigment (Bothast and Fennell, 1974; Assante et al., 1981). In addition, aflatoxigenic molds produce blue and yellow fluorescence on coconut extract agar (CEA) (Gourama and Bullerman, 1995). Nash Snyder medium (NS) and modified Czapek-Dox (MCz) medium are good media for detecting *Fusarium* species (Bullerman and West, 1990). Also, dichloran glycerol 18% agar (DG18) with 0.95 a_w or malt extract yeast extract 50% glucose agar (MY 50G) with 0.89 a_w can be used for detection of xerotolerant fungi (Samson et al., 1996). Since low-pH media can be harmful for fungal spores, the neutral-pH media in combination with antibiotics such as chloramphenicol, chlortetracycline, oxytetracycline, gentamicin, and streptomycin are used to detect fungi (Gourama and Bullerman, 1995).

2.2.4 Fungal volatiles

Different volatiles of *Aspergillus spp., Fusarium spp.,* and *Penicillium spp.* have been identified and can be used for detection and identification of fungal species (Borjesson et al., 1993, Zeringue et al., 1993). Common volatiles are 2-methyl-1-propanol, 3-methyl-1- butanol, 1-octen-3-ol, 3-octanone, 3-methylfuran, ethyl acetate, malodorous 2-methyl- isoborneol, and geosmin (Schnurer et al., 1999). Metabolic pathway for biosynthesis of the main fungal volatile metabolites is given in Fig. 2.1. Selected ion flow tube-mass spectrometry (SIFT-MS) method (Fig. 2.2) is based on the chemical ionization of volatile compounds and can be used for detection of reactive volatile compounds with low molecular weight produced by *A. flavus, A.*

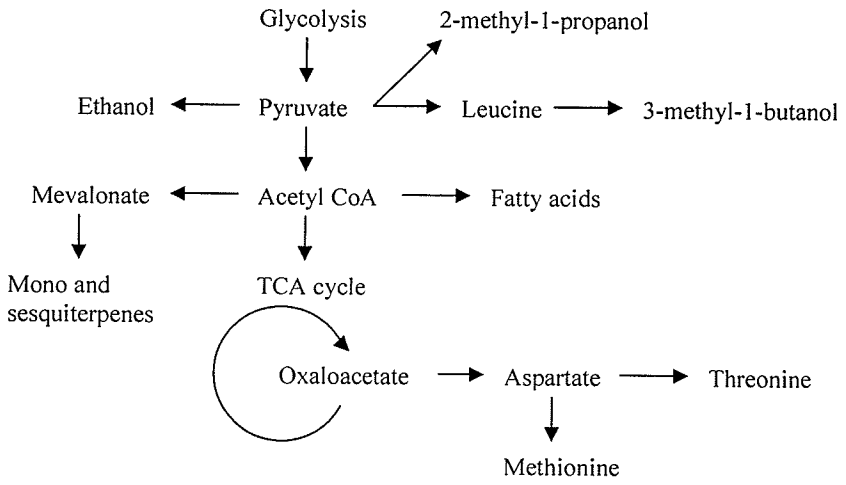

Fig. 2.1 Metabolic pathways for biosynthesis of the main fungal volatile metabolites (Larsen (1997) cited by Schnurer et al. (1999))

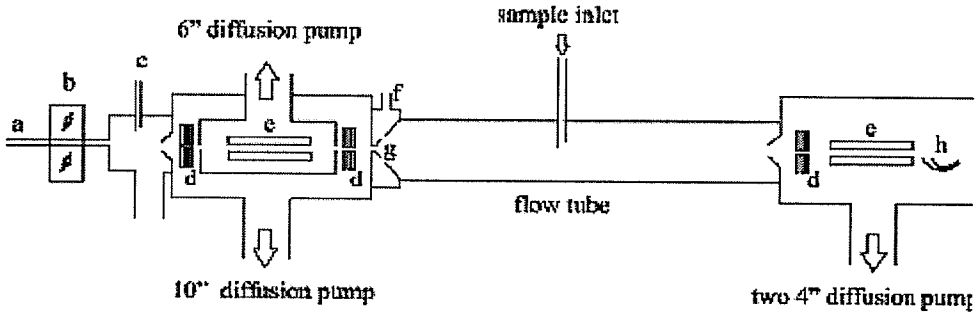

Key to Figure
a. Flowing afterglow He inlet.
b. Microwave discharge.
c. Flowing afterglow ion precursor gas inlet.
d. Electrostatic lens elements.
e. Quadrupole mass filter.
f. Flow tube He inlet via Venturi orifice.
g. Venturi injection orifice.
h. Continuous dynode-type particle multiplier.

Fig. 2.2 Schematic diagram of the SIFT-MS set up (Scotter et al., 2005)

fumigatus, Candida albicans, Mucor racemosus, F. solani, and *Cryptococcus neoformans* (Scotter et al., 2005). Although real time quantitative monitoring can be used in this method, the production of volatile compounds highly depends on the culture medium, e.g., carbohydrate-rich media gave the maximum quantity of volatile compounds.

2.2.5 Electrical impedance method

In this method, change in impedance of a medium is measured since it is highly correlated with a level of conidia, i.e., immotile vegetative tissue of fungi (Jarvis et al., 1983). For food samples, antibiotics should be used to prevent the growth of bacteria and other microorganisms. Also, detection time decreases when there is a large number of colonies present on the medium.

2.2.6 Immunological methods

Immunological methods have been used for the detection of fungal infection in food and feed since 1973 since there is a correlation between antigens and mycelial growth (Notermans et al., 1986). In this method, fluorescent antibody conjugate or fluoroscent dye linked with fungi specific antibody is applied to the sample which is observed directly under the microscope in UV light. It becomes fluorescent if a specific antigen is present. It is possible to detect *Alternaria, Aspergillus, Penicillium* and *Fusarium* species in grain (Hornok and Jagicza, 1973; Warncock, 1973; Yong and Cousin, 2001). An enzyme-linked immunosorbent assay (ELISA) can be used to detect the antigens separated from *Penicillium* spp., *Mucor* spp., *Cladosporium* spp., *Fusarium* spp., and *H. lanuginose* (Notermans and Heuvelman, 1985; Dewey et al., 1992). Mold latex immunoaggutination kit developed by Holland Biotechnology

(HBT, the Netherlands) can detect *Aspergillus* spp. and *Penicillium* spp. reliably and quickly (Kamphuis et al., 1989; Notermans and Kamphuis, 1992). In this method, latex beads are coated with immunoglobulin and they form a glue-like complex after coming in contact with extra cellular polysaccharides.

2.2.7 Most probable number (MPN) method

Dilution series of samples are made and the growth of microorganisms is observed and compared with the most probable number (MPN) table (Oblinger and Koburger, 1975). Quality Assurance (QA) Laboratories Limited designed the hydrophobic grid membrane filters (HGMF) on the principal of MPN method which had a grid made up of 1600 growth compartments of agar. It was more efficient than traditional methods, required less media, glassware, and time; and it could enumerate the molds but it could not identify species of mold. Also, it was hectic and time-consuming for a large number of samples. Therefore, HGMF was automated by using a black and white camera and a computer (Brodsky et al., 1982). Since each colony produces different colour, automated HGMF can differentiate between the species.

2.2.8 Polymerase chain reaction (PCR)

Polymerase chain reaction (PCR) is a biochemical and molecular-biological technique for isolating sequence of Deoxyribo Nucleic Acid (DNA). Certain genes are responsible for aflatoxin production, e.g., aflR1 and afl-2 (Payne et al., 1993). PCR is highly sensitive for aflR1 and therefore, *A. flavus* and *A. parasiticus* can be easily detected (Manonmani et al., 2005) but it is hardly sensitive for lower concentrations of fungal infection (Farber et al., 1997).

2.2.9 Howard mold count (HMC)

Howard mold count (HMC) has been in use for 90 years as the universal standard for mold assessment (Magan, 1993). It is a direct method and in this method, slides of material are inspected through microscopes for the presence of fungi. It is commonly used for fungal detection in tomato. Fungal fragments present in the sample indicate the presence of fungi and possible presence of mycotoxins.

2.2.10 Image analysis

Electromagnetic radiation can be described as a stream of photons, each traveling in a wave-like pattern, moving at the speed of light and carrying some amount of energy. The energy spectrum includes radio waves, microwaves, terahertz radiation, infrared radiation, visible light, ultraviolet radiation, X-rays, and gamma rays. Photon energy increases in ascending order from radio waves to gamma rays as shown in Fig. 2.3. The amount of energy of a photon makes it behave like a wave and sometimes like a particle. This is called the "wave-particle duality" of light. Low-energy photons (e.g., radio waves) behave more like waves, while higher energy photons (e.g., X-rays) behave more like particles.

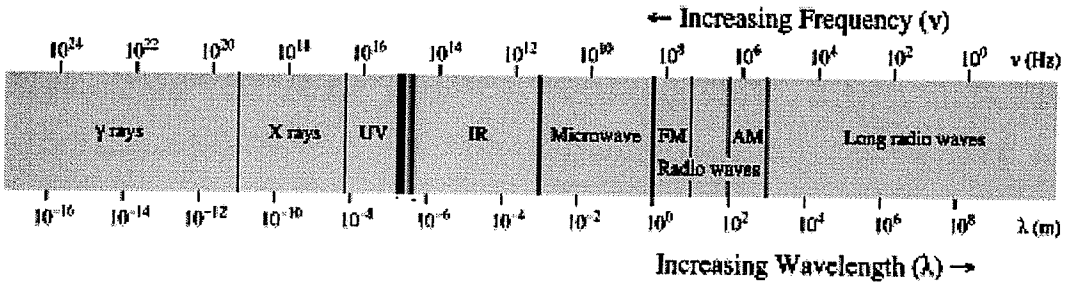

Fig. 2.3 Electromagnetic Spectrum (Wikimedia Foundation Inc., 2007a)

Different frequencies can be used for the detection of fungal growth. Visible spectra can correctly classify corns into healthy and infected kernels with 82.5% accuracy (Pearson and Wicklow, 2006) while Ordaz et al. (2003) used natural fluorescence of aflatoxin to detect aflatoxin producing species using ultraviolet (UV) light but UV lights failed to identify the species of fungi. Ultrasound signals are inversely related to the level of fungal infection ($r^2 = 0.85$) (Walcott et al., 1998).

A unique chemical composition causes molecules to absorb near infrared (NIR) light and vibrate at specific frequency (Murray and Williams, 1990). Near infrared (NIR) can excite and overtone the molecular vibrations to high energy levels. Transmittance and reflectance spectra can detect fungal infection with 81 to 98% accuracy (Pearson et al., 2001; Delwiche, 2003; Pearson et al., 2004; Wang et al., 2004; Pearson et al., 2006; Singh et al., 2007) but this method hardly does not work for 10-100 ppb aflatoxin concentration. Also, this method has a difficulty to classify different species of fungi (Delwiche, 2003). Mass and density of infected kernels are lower than healthy kernels (Pearson et al., 2006). Therefore, X-rays can be used to detect fungal infection. Pearson et al. (2006) detected fungal-infected corn kernels by a soft X-ray method with 82% accuracy.

2.3 Advantages and Limitations of the Detection Methods

The above listed methods have their own limitations and not a single method can be generalized for detection of all types of fungi. Chemical methods are accurate but they are time consuming due to sample preparation and long observation duration. Since chitin is a cuticular component of insects also, it creates confusion in the results while separation of fungal ATP from plants' and other microorganisms' ATP is difficult.

Therefore, these techniques are not popular for fungal detection in food. The ergosterol method is a quick, easy, and sensitive indicator of fungal infection (Seitz et al., 1979) but it cannot differentiate between species of fungi. A lot of work is done in detection of fungi using media culture. Also, this method is easier, quicker, and more economical than the chemical methods for detection of mycotoxigenic fungi but it is difficult to find the right medium for a given species. The use of electrical impedence method is also limited due to its medium-sensitivity, e.g., a bactometer B32 can detect *A. ochraceus* at its maximum efficiency only with Blakeslee's malt extract agar (Williams and Wood, 1986). In addition, electrical impedance may vary with the ionic solutes and pH of the medium. In the immunoassay method, the quantification of molds and their growth levels is difficult (Hornok and Jagicza, 1973; Warncock, 1973).

Mold latex immunoaggutination kit is faster but less sensitive than ELISA (Kamphuis et al., 1989). Also, the possibility of false positive is high and it requires purification of samples (Manonmani et al., 2005). Immunoassay method can also be used for detection of metabolic byproducts of fungi (Notermans et al., 1986). This method is better than thin layer chromatography since antigens can be detected earlier than aflatoxins.

Most probable number (MPN) method is more accurate, reliable, and quicker than the conventional aerobic plate method and can detect fungi even when they are small in number (Hastings et al., 1984), but it needs skilled personnel. Polymerase chain reaction (PCR) method is quicker, more sensitive, and more flexible than ELISA (Arnheim and Erlich, 1992) but it cannot detect probable invasion (White et

al., 2005). Also, the fat, protein, and carbohydrate content in the foods can interfere in analysis. Howard mold count (HMC) method cannot identify fungi. Also, the slide preparation is time consuming and it requires skilled persons.

Use of the energy spectrum in the detection of fungal infection need little sample preparation and reduces detection time and human labour. Near infrared (NIR) spectroscopy can be used for detection of infection in bulk sample but a X-ray method is preferred when the number of infected kernels is required because the infection level in the soft X-ray method is measured by counting the number of infected and healthy kernels whereas in the NIR spectroscopy, infection is measured by determining the mass of infected and healthy kernels (Karunakaran et al., 2005).

2.4 X-rays

X-rays are used to observe underlying tissues and internal defects. In 1895, a German physicist (Roentgen) discovered X-rays and named them Roentgen rays. He called them X-rays because of their unknown nature at first (The Columbia Electronic Encyclopedia, 2007). In a vacuum, X-rays travel in a straight line in the form of waves and are undetectable to the naked eye. X-rays are a form of ionizing and electromagnetic radiation with wavelength in the range of 0.1 to 100 nm and frequency in the range of 30×10^{15} to 30000×10^{15} Hz (Wikimedia Foundation Inc., 2007b.).

When X-rays pass through an object, they strike a photographic plate or a fluorescent screen. The darkness of the shadows produced on the plate or screen depends on the relative density of different parts of the object and it results in a visual

image of the interior structure. Photographs made with X-rays are known as radiographs or skiagraphs. X-rays are divided into two classes, hard X-rays and soft X-rays, on the basis of their energy level. Hard X-rays have higher energy (up to 300 keV) than soft X-rays (up to 10 keV) (Kylafis, 2005). Hard X-rays also have higher frequency, shorter wavelength, higher penetration power, and higher intensity than soft X-rays.

2.4.1 Production of X-rays

2.4.1.1 X-ray tube

An X-ray tube consists of two electrodes, a cathode and an anode (Fig. 2.4). X-rays are produced by two different processes (The Columbia Electronic Encyclopedia, 2007). In the first process, radiation is emitted by electrons themselves when their speed is lowered while passing near the positively charged nuclei of the anode material. The kinetic energy of electrons is converted into photon energy which is given by the Eq. 2.1.

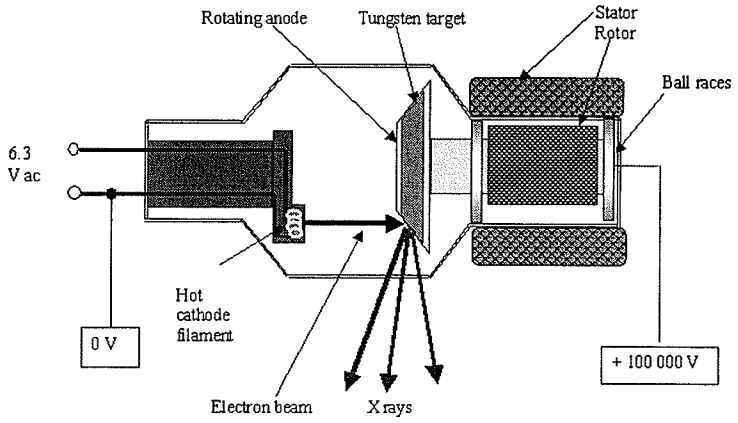

Fig. 2.4 Schematic diagram of X-ray tube (Anonymous, 2007)

$$eV = \frac{hC}{\lambda} \tag{2.1}$$

where,

e = Charge of electron, 1.6×10^{-19} C,

V = Voltage, V,

h = Planck's constant, 6.6×10^{-34} Js,

C = Speed of light, 3×10^{8} m/s, and

λ = Wavelength of radiation, nm.

In this process, X-rays are produced in the continuous frequency range.

The minimum wavelength of X-rays is given by Curry et al. (1990) (Eq. 2.2).

$$\lambda \min = \frac{1.24}{Voltage\ in\ kV} \tag{2.2}$$

X-ray approaches are most likely to be successful when the X-ray absorption in the defective area is different from that in healthy area. The intensity of X-rays is given by Richards et al. (1960):

$$I = I_0 e^{-\mu_{av} X} \tag{2.3}$$

where,

I = Intensity of the transmitted beam, $Jm^{-2}s^{-1}$,

I_0 = Intensity of the incident beam, $Jm^{-2}s^{-1}$,

μ_{av} = Average linear absorption coefficient of the medium, m^{-1}, and

X = Thickness of the medium, m.

$$\mu = k\rho Z^3\lambda^3 \quad (2.4)$$

where,

k = Constant parameter,

ρ = Density of the material, kgm^{-3},

λ = Effective X-ray wavelength, m, and

Z = Effective atomic number.

In the second process, a high voltage between the electrodes causes the accelerated streams of electrons (cathode rays) from the cathode to the anode and produce X rays in a discrete frequency range as they strike the anode. Tungsten, alloys of tungsten, rhenium, copper, and cobalt are commonly used as anodes while molybdenum is used for specialized applications (The Columbia Electronic Encyclopedia, 2007).

2.4.1.2 Synchrotron

A synchrotron is a particle accelerator in which electric and magnetic fields are synchronized with the moving particles (Fig. 2.5). When accelerated particles move in a curved trajectory in the presence of magnetic field, X-rays are produced tangentially to the trajectory path (Attwood, 1999).

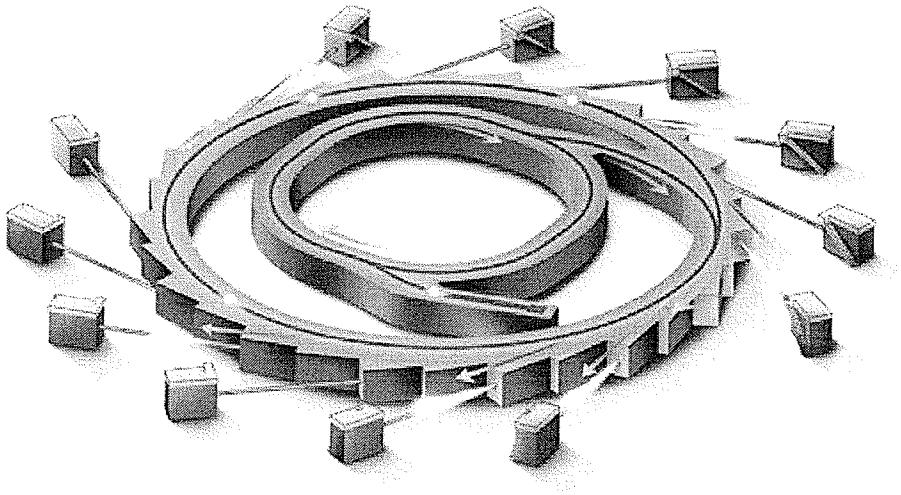

Fig. 2.5 Schematic diagram of Synchrotron (Monash University, 2003)

2.4.2 Applications of X-rays

Soft X-rays are mainly used for non-destructive detection of internal defects in a material. Most of the applications of X-rays depend on their penetration ability, energy, intensity, and the type of material. The intensity of the X-rays exiting the product depends on the incident energy, atomic number, and absorption/attenuation coefficient, and density and thickness of the product. X-rays mainly detect variations in density, mass, and the quality parameters associated with them. The density and thickness of agricultural produce changes with maturity and vigor. Therefore, soft X-rays can be used for quality control of agricultural produce. Due to the high moisture content in fruits and vegetables, water dominates X-ray absorption (Tollner et al., 1992; Shahin and Tollner, 1997; Abbott, 1999) but the moisture content has no significant effect on the classification accuracy of grain. Soft X-rays can be used to detect sprouting and virtuousness of wheat kernels (Neethirajan et al., 2006b, 2007a). Vitreous kernels have high grey value and larger area than non vitreous kernels (Neethirajan et al., 2006b). The classification accuracy of dual energy X-ray imaging

was higher than simple transmission X-ray imaging (Neethirajan et al., 2007b). Soft X-rays can be used for flow rate measurement of grains and chemicals which is important for designing handling equipment. Flow rate measurement is related to the attenuation coefficient of material which depends on its density and atomic number. Information can be extracted from a thin slice of sample by evaluating the cross section of an object using a movable X-ray source and detector set up in computerized axial tomography (CAT) (Sonego et al., 1995). Neethirajan et al. (2004) studied orientation, length, and area of air flow path using a soft X-ray CT scanner to find the reason behind the higher values of vertical air flow resistance than horizontal air flow resistance in the bulk grain. It was difficult to find out the orientation of kernels using CT scan images. Hence, visible images were studied which showed that kernels tend to lie horizontally. From CT scan images, it was found that there was only 9% difference between horizontal and vertical air flow paths. X-ray CT numbers can be used to represent the X-ray absorption characteristics which differentiate the food and foreign materials, but application of this method is limited to small particles only (Ogawa et al., 1998). X-ray method can detect live or dead insects, fractures or cracks in grains, infected kernels, and bones in deboned poultry (Chen et al., 2001). This method is being used extensively in flour mills in the US for detecting insect infection (Schatzki and Fine, 1988).

2.4.2.1 Detection of internal defects in fruits and vegetables

X-ray imaging is the most sensitive and effective method to detect structural discontinuities and density differences inside the material (Ogawa et al., 1998; Bowers, 1989). X-ray machines are commercially in use for detection of hollow hearts in potatoes (Rex and Mazza, 1989). The internal cavity of the potato is highly

correlated with the second derivative of the X-ray density curve (r^2 = 0.97) (Finney and Norris, 1978). The X-ray density (D) is the measure of a density curve and it is calculated by Eq. 2.5.

$$D = \log\frac{X1}{X2} \tag{2.5}$$

where,

X1= Quantity of X-rays measured without potato

X2= Quantity of X-rays measured with potato

The second derivative of density curve cannot detect splits in peach because of their non uniform cross-section. Therefore, the detection algorithm was developed on the basis of maximum and minimum intensities for each individual peach and then the pit area was isolated by calculating threshold value (Han et al., 1992). The algorithm could detect 98% of the healthy peaches correctly. Though X-ray absorption for all the cultivars was almost the same, there was a considerable effect caused by the orientation of peaches on the absorption of X-rays.

In certain apple cultivars, watercore is a serious internal problem which results in death of surrounding tissue and internal browning. This fluid replaces voids in the tissue, making bruised apple denser than healthy apple. The density of healthy apple ranges from 0.699 to 0.850, while the density of watercore apple is up to 1.1 (Fiedler et al., 1973 cited by Kim et al., 2000). Therefore, soft X-rays can sort out watercore apples from healthy apples with 5-8% false positive to negative ratio (Schatzki et al., 1997; Kim et al., 2000). Similarly, density of a lettuce head increases with maturity

and hence, penetration of X-rays decreases. Lenker and Adrian (1971) used this fact in their design of a mechanical harvester for lettuce heads in which an X-ray sensor was used. The mechanical harvester picked only 4% soft lettuce compared to 13% soft heads picked by experienced workers. The X-rays can also be used to determine the maturity stage of tomato and peach (Lenker and Adrian, 1971; Brecht et al., 1991; Barcelon et al., 1999).

Detection of spongy tissue in Alphanso mango is very difficult with the naked eye due to lack of external symptoms. It is a ripening disorder in which fissures and air cavities are observed in the tissue. Since healthy tissue is denser than affected tissue, absorption coefficient of X-rays is higher in healthy tissue than diseased tissue (Thomas et al., 1993). In the X-ray images, the spongy tissue and healthy tissue can be recognized by dark grey and light grey color, respectively. The results obtained from X-ray photography and those from internal detection of cut fruits were highly correlated. X-ray imaging can classify healthy and poor quality onions with 90% accuracy on the basis of their rigidity (Shahin et al., 2002). Onion bulbs consist of continuous and concentric layers of laminae starting from the base. The laminae in diseased onions are not as rigid as in healthy onions due to the change in density and water content. These physiological changes appear in the form of expanded boundary and radial bar defects in X-ray images (Tollner et al., 1995 cited by Shahin et al., 2002). X-rays can also indicate sprouting in onions by detecting altered moisture distribution in the center of the bulb (Shahin et al., 2002).

2.4.2.2 Detection of internal infections in grain

Early detection of infection is very important in grain storage to reduce the storage losses. Trained persons can recognize external infection with only 80% accuracy which increases exponentially with maturity of insects (Keagy and Schatzki, 1991). X-rays were used for the first time in 1932 for detection of pink bollworm in cotton seeds (Fenton and Waite, 1932). However, X-rays also can be used to study the developmental stages and behavior of insects without dissecting the grains (Pederson and Brown, 1960; Mills and Wilbur, 1967; Sharifi and Mills, 1971a, 1971b). Density of healthy kernels is different from infected kernels. Stermer (1972) used an aqueous solution of potassium carbonate (K_2CO_3) to enhance this density difference which fills voids and produces opacity under influence of vacuum. Use of K_2CO_3 improves accuracy of the X-ray method up to 90% in early stages (egg and small larvae) of infection and up to 100% in kernels infected by pupae and adults. Sometimes mechanically damaged kernels can be identified as infected kernels due to the chemical entry into the kernel while sometimes the chemical cannot enter due to the blocked egg holes. Analog X-ray film images, obtained at 12 to 30 kV potential and 8 to 10 mA current for 3 to 5 s, can detect all the stages of internal infection and estimate the extent of losses (Milner et al., 1950). Currently, digitized X-ray imaging is being used for detection of internal infection in grain (Keagy and Schatzki, 1993) which not only detects and identifies insect species but also determines a life stage of the insect by comparing image features (Karunakaran et al., 2004a, 2004b; Fornal et al., 2007). Though film imaging gives more accurate results than digital imaging, analysis of film images is hectic, subjective, and time consuming (Milner et al., 1952; Haff and Slaughter, 2002). Initial cost of digital imaging is higher than film imaging but it reduces cost of film and film developing (Haff and Slaughter, 2002). Haff and

Slaughter (2004) employed real time X-ray imaging for detection of granary weevil in wheat which could accurately detect 84.4% of infected kernels while the accuracy of film imaging was 90.2%. Long time exposure of kernels to X-rays in film imaging is beneficial in detecting early stages of infection. The youngest insects cannot be detected by digital image analysis. Therefore, real time X-ray imaging is useful only if the grain has been in storage for several months. The soft X-ray method has potential to detect fungal infection in grains (Pearson and Wicklow, 2006) since healthy kernels are denser than fungal damaged kernels. Therefore, healthy kernels produce darker images than fungal-infected kernels.

2.4.3 Hazards of X-Ray use

X-rays ionize the matter by ejecting electrons from their atom. X-rays are measured by two types of survey meters, Geiger counter and ionization chamber. The Geiger counter counts individual photons while the later counts ion pairs produced by radiation. Ionization and absorption of X-rays depend on radiation flux, intensity, and photon energy of radiation and the nature of the material. Ionization is measured in a standard unit Roentgen (R) while absorption is measured in rad (Roentgen absorbed dose), rem (Roentgen equivalent man), and Gray (1Gy = 100 rem). Though X-ray absorption up to 0.5 mGy/yr by living organism is harmless, large dose in short exposure may result in tissue damage, e.g., reddening or destruction of skin (Jerkins and Haas, 1973). The maximum permissible dose equivalent is 20 mGy/yr for radiation workers and 1 mGy/yr for a common person (International Commission on Radiological Protection, 1990). In regular life, common man is exposed to 0.02-1.74 mGy/yr due to natural radiation, colour television, and medical X-rays (Robertson, 1976). A worker operating a real-time automatic X-ray inspection system is exposed

to 7.2 mGy/yr which is much lower than the maximum permissible level for radiation workers (Robertson, 1976). The operator should wear finger or wrist type radiation monitoring devices. The amount of radiation on the whole body can be measured by wearing monitoring devices on chest or abdomen. When the film badge is worn at proper height and facing the radiation source, it records an exposure history for a person. This badge should be changed in 2-4 weeks cycles (Jerkins and Haas, 1973).

Irradiation is used on agricultural produce to control infection and food spoilage. The World Health Organization declared that food irradiated with a dose of 10 kGy is safe for consumption but exposure of cereal grains to the X-rays higher than 3-5 kGy can cause major damages to the processing quality. X-rays can also cause mutation in seeds on exposure to high levels (Belcher, 1968 cited by Schnurer et al., 1999). The maximum permissible X-ray dose for cereal grains is 0.75 kGy in Canada (Banks and Fields, 1995). In practice, X-ray inspection system exposes the grains to less than 0.1 Gy X-ray doses (Tollner, 1993). Haskin and Moore (1935) observed premature flowering, discolouration, duplication, and twisting in citrus exposed to 3-13 Gy of radiation. On the other hand wheat kernels exposed to 0.6 to 1.14 Gy showed accelerated growth rate and an increase in weight (Wort, 1941).

2.4.4 Data analysis

Image analysis is usually performed to extract meaningful information from images and it includes three main steps which are explained below:

2.4.4.1 Image acquisition

In digital radiography, digital images are obtained either by digitizing the analog images using a digitizer or frame grabber or by converting X-rays into light which is captured by a light sensitive digitizing system. In fluoroscopy, the photographic plate is replaced by a fluorescent screen. It is advantageous over radiography in terms of cost and time but images obtained have less sharpness. Information can be extracted from a thin slice of sample by evaluating the cross section of an object using a movable X-ray source and detector set up in computerized axial tomography (CAT) (Sonego et al., 1995). Large variations in sample thickness can be placed in one range by keeping the voltage and current of the X-ray tube at minimum. This can also be helpful in obtaining good resolution (Thomas et al., 1993). An automated X-ray detector for grain inspection requires image resolution of 65 μm or smaller (Keagy and Schatzki, 1991). Different combinations of voltage and current are listed in Table 2.1. Crease down view of a grain kernel is the most promising view (Myers and Edsall, 1989) while it is difficult to place a grain kernel for side view (Barker et al., 1992).

Table 2.1 Reported combinations of current and voltage used for image acquisition.

Crop	Application	Current (μA)	Voltage	Resolution (μm)	Time (s)	Reference
Wheat	Granary weevils	99000	12keV	100	0.149	Haff and Slaughter (2002)
Wheat	*Rhyzopertha dominica, Tribolium. castaneum*	65	15 kV	16.7	3-5	Karunakaran et al. (2004a), Karunakaran et al. (2004b)
Wheat	*Sitophilus granarius L.*	60	20 kV	0.127mm^2/pixel	120	Fornal et al. (2007)
Wheat	*Sprouted kernels*	185	13.5 kV	62.5	3-5	Neethirajan et al. (2007)
Corn	*Fungal infected kernels*	3000	18 kV	31.7	120	Pearson and Wicklow (2006)
Wheat	*Vitreous and non-Vitreous kernels*	65	17 kV	16.66	3-5	Neethirajan et al. (2006)
Rice	*Cracks*	8000	12 keV	127	10	Kumar and Bal (2007)

2.4.4.2 Feature extraction and selection

Segmentation is a process of dividing a digital image into multiple regions of interest to extract more meaningful information for the further analysis. Thresholding method is commonly used for segmentation (Karunakaran et al., 2004a, 2004b; Neethirajan et al., 2006a; Kumar and Bal, 2007). Analysis of a segmented image is then aided by extracting useful quantitative attributes, i.e., features which can be classified into external and internal features (Pavlidis, 1980). External image features are derived from the boundary co-ordinates of an image while internal image features are extracted from the properties of pixels inside the boundary. External features include morphological features that describe shape, e.g., Fourier descriptors, wavelet transforms, boundary chain codes and internal features take account of textural features, moments, colour. Since external features are not sufficient for high performance inspection, they need to be combined with internal features for classification of grains (Luo et al., 1999; Paliwal et al., 1999). Statistical measures of shape of an image are provided by spatial moments while colour features represent brightness of an image (Jayas et al., 2000). Similarly, textural characteristics of an image such as granulation, smoothness, roughness, fineness, coarseness, and randomness can be shown by textural features on the basis of distribution of colour with respect to spatial coordinates (Gonzalez and Woods, 1998). Selection of the best representing features is very important for best classification results (Jayas et al., 2000). For illustration, external features are important for classification of kernels into different varieties (Paliwal et al., 2005) but internal features are important for detection of infection and virteousness (Karunakaran et al., 2004a, 2004b; Neethirajan et al., 2006). Principal component analysis is a popular technique in feature selection that compresses the data of high dimensional vectors into low dimensional vectors in

terms of least mean square error. Computer programs written in MATLAB (The MathWorks Inc, Natick, MA) or SAS can be used for feature extraction and selection.

2.4.4.3 Classification

The objects can be classified according to the extracted features either by statistical classifiers or multi-layer neural networks (MLNN). Barker et al. (1992) used parametric and non-parametric methods for pattern recognition of eight Australian wheat varieties. Parametric methods can be used if there is multivariate normal within-class distribution otherwise it is advised to use non parametric methods (Jayas et al., 2000). It was found that non-parametric methods made samples more consistent and hence, performance of classifier was improved. Neethirajan et al. (2006b) used and compared quadratic function parametric classifier and non-parametric Bayesian classifier for identification of vitreous and non-vitreous kernels. It was found that Bayesian classifier performed better than quadratic function parametric classifier. Shahin and Tollner (1997) used fuzzy logic on the X-ray images of water-core in apples and separated three different watercore levels with 64% accuracy. These results were improved up to 79% accuracy by applying Bayesian classifier with global (spatial and transform) features such as discrete wavelet transform (DWT) and discrete cosine transform (DCT) (Shahin et al., 1999).

Jayas et al. (2000) stated that MLNN facilitates with adaptively, fault tolerance, and massive parallel processing could be used as an alternative to statistical methods in classification and identification of agricultural products. It was also stated that back propagation neural network (BPNN) performs best in grain discrimination. Patel et al. (1996) trained neural network models using extracted features from gray

scale images of eggs and classified the eggs into eggs with blood spot and eggs with dirt stains with an accuracy of 85.6 and 80.0%, respectively. Karunakaran et al. (2004a, 2004b) tested BPNN and statistical classifiers. Back propagation neural network (BPNN) performed better than parametric and non parametric statistical classifiers for *Rhyzopertha dominica* but there was no significant difference between the performance of BPNN and statistical classifiers for *Tribolium castaneum*. Neethirajan et al. (2007) found that the BPNN had better accuracy (90 and 95% for sprouted and healthy kernels, respectively) than that of statistical classifiers (87 and 92% for sprouted and healthy kernels, respectively). Wang et al. (2004) classified soybean kernels into healthy and damaged kernels by using a diode array NIR spectrometer with the help of a partial least square model and artificial neural network (ANN) model with 93.5 to 94.6% accuracy.

To summarize, the X-ray method is a multitask system which can be used with statistical classifiers and MLNN for detection of internal disorders, infection, vitreousness as well as sprouting.

3. MATERIALS AND METHODS

The experiments were conducted to assess the capability of a soft X-ray method to detect infection in stored wheat due to *Aspergillus niger, A. glaucus,* and *Penicillium* spp. using different statistical and neural network classifiers. The main steps of the experiment are as shown in Fig. 3.1.

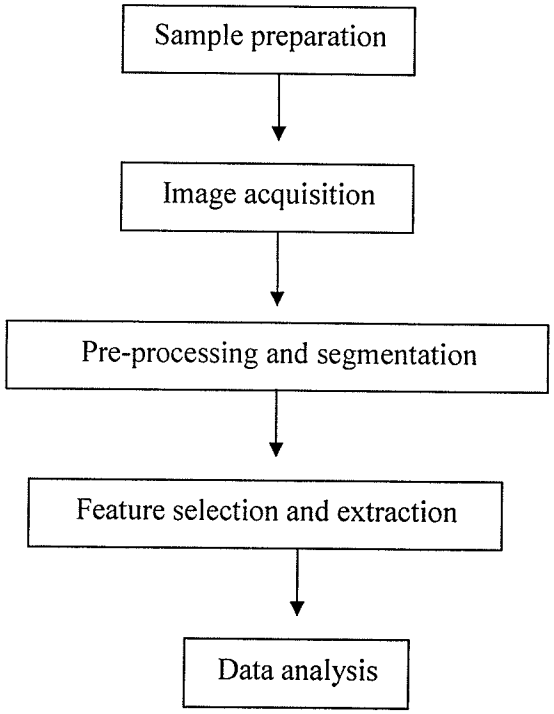

Fig. 3.1 Flow-diagram of X-ray image analysis

3.1 Sample Preparation

Samples of wheat kernels infected with *A. glaucus, A. niger,* and *Penicillium* spp. were prepared separately at the Cereal Research Centre, Agriculture and Agri-Food Canada, Winnipeg, Manitoba, Canada. The wheat kernels infected with fungal species were plated on filter paper saturated with 7.5 mL aqueous NaCl in petri dishes for one week. Then pure fungal lines of *Aspergillus* spp. and *Penicillium* spp. from infected kernels were placed on potato dextrose agar (PDA) for seven days at 30°C and 10°C, respectively. After that PDA with fungi was placed in a plastic spray bottle containing 200 ml sterilized water with one drop of Tween 20 and the whole mixture was shaken up to prepare the fungal solution. A 20 kg sample of Canada western red spring (CWRS) wheat (cv. AC Barrie) with 17% moisture content (wet basis) was surface sterilized by soaking in 1% sodium hypochlorite for 2 min. The wheat kernels were thoroughly washed using sterilized water and then placed on paper towel for 2 h. For each fungus, about 1 kg of moistened wheat, placed a few layers deep in a large plastic tub, was misted with the fungal solution in a fume hood and covered with a loose plastic bag for 8 weeks at 30°C. Each sample in a fume hood was shaken up for 1 min in four plastic bags sequentially and poured into a fifth plastic bag before imaging to simulate the process of mixing of grain during handling. All the samples were air-dried to reduce their moisture content to 15% (dry basis) which was then measured using the oven-dry method.

3.2 Image Acquisition

The main components of X-ray imaging system (Fig. 3.2) were 1. Lixi fluoroscope (LX-85708, Lixi Inc., Downers Grove, IL); 2. CCD black and white camera (Sony XC-75/75CE); 3. black and white monitor; and 4. image digitizer (TV@Anywhere

Plus, MSI: S36-0000311-K45, Taiwan, China). A single kernel image of 300 wheat kernels from each fungal infected sample (*A. glaucus, A. niger* and *Penicillium* spp.) and 300 kernels of healthy kernels were acquired with 62.5 μm screen resolution using the Lixi fluoroscope that consisted of X-ray tube, X-ray detection system, and power supply unit. X-ray tube and X-ray detection system were 12.7 mm and 25 mm in diameter, respectively, and they were encased in the stainless steel cabinet with X-ray shield for safety. The current and voltage of the X-ray tube could be adjusted in a range of 0-200 μA and 0-50 kV, respectively, with the help of control knobs provided on the power supply unit. The combination of 13.6 kV voltage and 184 μA current was fixed for image acquisition of wheat kernels by conducting the preliminary experiments. The wheat kernels to be X-rayed were manually placed in crease down position on the XY motorized manipulator (saran wrap) situated between the detector and X-ray tube. X-ray image of a single kernel at a time was then acquired by adjusting its position in the centre of screen with the press buttons provided on the cabinet to move the saran wrap in horizontal and vertical directions. Analog images were digitized into 8 bit gray scale images at 60 pixels/mm resolution using a capture card called TV@Anywhere Plus (MSI: S36-0000311-K45, Taiwan, China). Digital images were stored in a personal computer for further analysis.

3.3 Pre-processing

Images obtained were cropped manually. The grey level was not constant throughout the image. Also, the background and kernel had some grey levels in common.

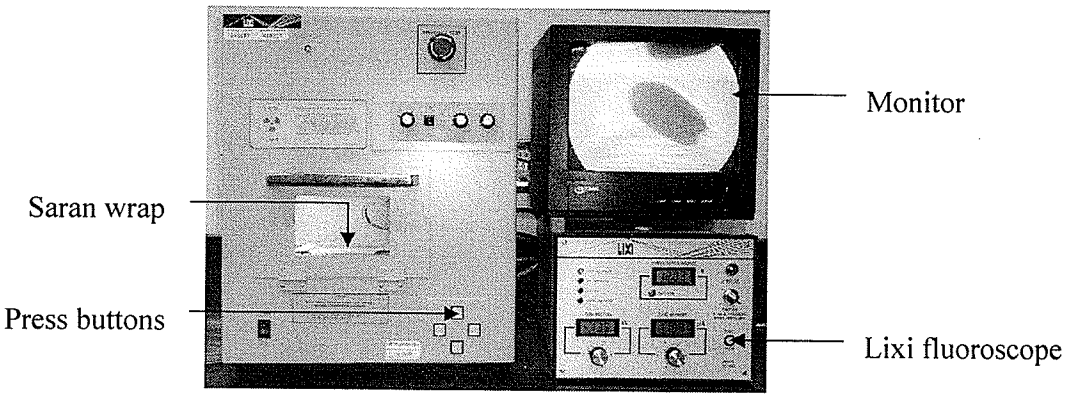

Fig. 3.2 Experimental set up

Therefore, it was difficult to remove a kernel from the background without losing any information from the kernel by a simple thresholding method. Hence, the kernel was separated from the background using *bwlabel* MATLAB (The Mathworks Inc., Natick, Mass.) function which returns a matrix of original image size but label only the kernel i.e. the connected objects (4 or 8 neighbours) excluding the background.

3.4 Feature Selection and Extraction

Healthy kernels vary from fungal-infected kernels in density (Pearson et al., 2006). Also, changes in the textural properties of grain surface such as smoothness, coarseness, fineness, and granulation are observed due to fungal infection. These textural properties of healthy and infected kernels can be determined using a gray level co-occurrence matrix (GLCM). Therefore, a total of 6 first order statistical and 28 textural features were selected (Table 3.1) and extracted from soft X-ray images of wheat kernels applying an algorithm developed in MATLAB (The Mathworks Inc., Natick, Mass.) with the assistance of Chandra Singh.

Table 3.1 List of the features extracted from soft X-ray images of wheat kernels.

Number	Feature	Code
1	Maximum gray level	MaxGL
2	Minimum Gray level	MinGL
3	Mean Gray level	Mean
4	Median Gray level	Med
5	Standard deviation Gray level	Σ
6	Variance Gray level	V
7-10	GLCM Energy	GE1, GE2, GE3, GE4
11-14	GLCM Homogeneity	GH1, GH2, GH3, GH4
15-18	GLCM Contrast	GC1, GC2, GC3, GC4
19-22	GLCM Correlation	CR1, CR2, CR3, CR4
23-26	GLCM Mean	GM1, GM2, GM3, GM4
27-30	GLCM Entropy	GE1, GE2, GE3, GE4
31-34	GLCM Maximum Probability	GP1, GP2, GP3, GP4

3.4.1 Gray level co-occurrence matrix (GLCM)

A gray level co-occurrence matrix (GLCM) is a distribution of co-occurring gray scale values of pixels over an image at given offset. In other words, GLCM is an information of how often specific combinations of gray level values occur in an image. GLCM considers a relationship between two pixels, one as a reference pixel and another as a neighbour pixel, at a time. Neighbour pixel may be in 0, 45, 90, and 135° direction. Each pixel of an image, starting from upper left hand corner to lower right hand corner, gets a chance to be a reference pixel. If neighbour pixel is in the

right direction of the reference pixel then it can be represented as (1, 0) that means 1 pixel in x direction and 0 pixel in y direction (Fig. 3.3).

The following properties were calculated from the GLCM (MATLAB, The Mathworks Inc., Natick, Mass.; Majumdar and Jayas, 2000)

$$\text{Mean} = \sum_{i,j} i * P(i,j) \tag{3.1}$$

$$\text{Contrast} = \sum_{i,j} |i-j|^2 P(i,j) \tag{3.2}$$

$$\text{Correlation} = \sum_{i,j} \frac{(i-\mu_i)(j-\mu_j)\overline{P}(i,j)}{\sigma_i \sigma_j} \tag{3.3}$$

$$\text{Energy} = \sum_{i,j} P(i,j)^2 \tag{3.4}$$

$$\text{Entropy} = \sum_{i,j} P(i,j) \log (P(i,j)) \tag{3.5}$$

$$\text{Homogeneity} = \sum_{i,j} \frac{P(i,j)}{1+|i-j|} \tag{3.6}$$

$$\text{Maximum Probability} = \text{Max}\,(P(i,j)) \tag{3.7}$$

where,

$P(i,j)$ = Matrix of relative frequencies,

i, j = Gray levels,

μ_i, μ_j = Mean of i and j gray levels, and

$\overline{P}(i,j)$ = Joint probability occurrence of specified pixel pairs.

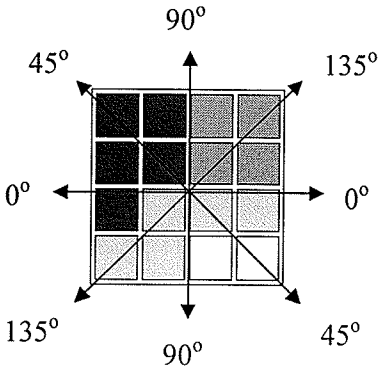

(a) Gray scale Image

0	**0**	**1**	**1**
0	**0**	**1**	**1**
0	**2**	**2**	**2**
2	**2**	**3**	**3**

(b) Matrix

Gray Level	Gray Level			
	0	**1**	**2**	**3**
0	4	2	1	0
1	2	4	0	0
2	1	0	6	1
3	0	0	1	2

GLCM (0° direction)

Gray Level	Gray Level			
	0	**1**	**2**	**3**
0	2	1	3	0
1	1	2	1	0
2	3	1	0	2
3	0	0	2	0

GLCM (45° direction)

Gray Level	Gray Level			
	0	**1**	**2**	**3**
0	6	0	2	0
1	0	4	2	0
2	2	2	2	2
3	0	0	2	0

GLCM (90° direction)

Gray Level	Gray Level			
	0	**1**	**2**	**3**
0	4	1	0	0
1	1	2	2	0
2	0	2	4	1
3	0	0	1	0

GLCM (135° direction)

Gray Level	Gray Level			
	0	**1**	**2**	**3**
0	16	4	6	0
1	4	12	5	0
2	6	5	12	6
3	0	0	6	2

Total GLCM

Fig. 3.3 Example of gray level co-occurrence matrix

3.5 Data Analysis

3.5.1 Statistical analysis

In the discriminant analysis, the groups and classification rule are predetermined from the training set and then tested with the test set. The discrimination classification method is based on Bayes classification rule that reduces a proportion of misclassified objects to minimise total error of classification (TEC), i.e., the probability of the misclassification of objects. Bayes criteria assign an object to a group with the highest conditional probability by Eq. 3.8 (Mitchell, 2006):

$$P(i|x) = \frac{P(x|i).P(i)}{\sum_{\forall j} P(x|j).P(j)} \tag{3.8}$$

where,

x = Set of measurement,

i, j = Groups into which objects are to be separated,

$P(i \mid x)$ = Probability of an object to belong to group i for x,

$P(x \mid i)$ = Probability of getting x of the objects from group i,

$P(x \mid j)$ = Probability of getting x of the objects from group j, and

$P(i)$, $P(\mathrm{j})$ = Prior probabilities of group i and j, respectively.

The classification accuracies of the statistical classifiers for fungal detection of wheat were tested using an algorithm developed in MATLAB (The Mathworks Inc., Natick, Mass.). For statistical classification, the sample set was divided randomly into independent training (240 kernels) and test (60 kernels) sets (true validation) and average results of three trials were reported.

3.5.2 Statistical classifiers

3.5.2.1 Linear discriminant analysis (LDA)

Linear discriminant analysis (LDA) is used when groups can be separated by linear combination of features. A separator may be a line for two features, a plane for three features or a hyper-plane for a number of features. It is assumed that the data have multivariate normal distribution and have identical covariance (pooled covariance) for each of the groups.

3.5.2.2 Quadratic discriminant analysis (QDA)

Quadratic discriminant analysis (QDA) is closely related to LDA but there is no assumption of identical covariance for each of the classes. A covariance matrix for each class is calculated separately.

3.5.2.3 Mahalanobis classification

Mahalanobis classifier uses mahalanobis distance, a multivariate measure of separation of data from a point in space, with stratified covariance estimates. It is useful to relate samples of unknown class to samples of known class. While using this method for classification of samples into different classes, a covariance matrix of each class is calculated from a training set and then, Mahalanobis distance of each sample in the test set is determined. Finally, a sample is classified into a class having minimum Mahalanobis distance.

3.5.3 Artificial neural network (ANN)

"An artificial neural network is a mathematical or computational model. It consists of an interconnected group of artificial neurons and processes information using the learning rule which is developed on the basis of external or internal information that flows through the network during the learning phase" (Wikimedia Foundation Inc., 2007c). Artificial neural network comprises of three types of neuron layers: input, hidden, and output layer. Eq. 3.9 describes the relationship between input and output layer (Gurney, 1997):

$$y = f(x) = K\phi\sum_{i=1}^{n}(w_i x_i - \theta) \tag{3.9}$$

where,

K = A constant,

ϕ = Nonlinear function,

w_i = Weight (i = 1,2,3,…,n, where n is the number of input variables),

x_i = Input variables, and

θ = Threshold value.

Number of hidden layers can be changed according to the requirement. The learning time, size of network, and the performance quality increases with number of hidden layers. Therefore, determination of an optimal number of hidden layers is very important for the best performance of ANN. Number of neurons in a hidden layer was determined by Eq. 3.10 (Neuroshell 2, version 4.0, Ward Systems Group, Frederick, MD):

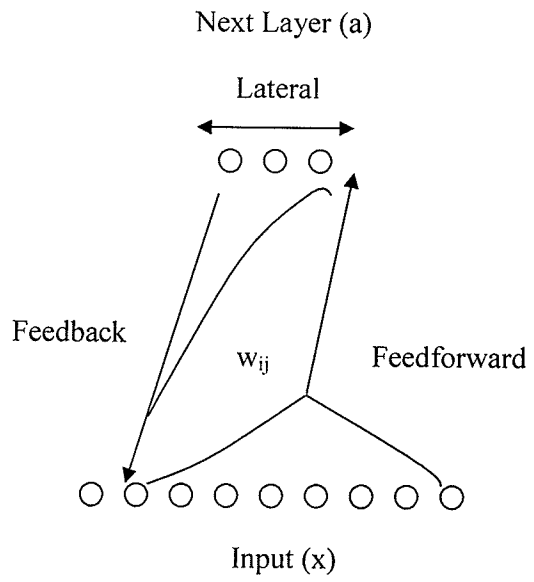

Fig. 3.4 Connections of Weight Building Box in ANN

$$N = \frac{Input + Output}{2} + Y^{0.5} \tag{3.10}$$

where,

Y = number of patterns.

Weight building blocks play an important role in conveying information from one layer to another. These building blocks can be connected in four different ways such as feed-forward, feedback, lateral, and time delayed connection (Fig. 3.4). Behaviour and performance of the neural network varies with the connections of building blocks.

In feed-forward connection, the data are forwarded from one neuron layer to the next without cycling while in feedback connection the data are transferred back to

the previous layer in cycles. Lateral connection allows the neurons to preserve a specific ordering relationship. Whereas time delay connection includes time delay elements and it is suitable for temporal pattern recognition. There are different types of ANN on the basis of number of layers, nodes, and types of connections such as back-propagation (BPNN), probabilistic, Kohonen, and general regression network (Neuroshell 2, version 4.0, Ward Systems Group, Frederick, MD). However, feedforward BPNN is suitable for discrimination of agricultural produce into different classes (Jayas et al., 2000).

The three layer back-propagation neural network was selected. There were two neurons in output layers and 34 neurons in input layer for pair-wise and two class classification models. The hidden layer consisted of 38 neurons as calculated by Eq. 3.10. Similarly, there were 4, 48, and 34 neurons in output, hidden, and input layers for four class classification model. The hidden and output layer had logistic function ($f(x) = 1/ (1+e^{-x})$) while the input layer had linear [-1, 1] function. All the layers of ANN had learning rate, initial weight, and momentum of 0.1, 0.3, and 0.1, respectively. Calibration interval (events) was fixed at 200 for the test set. The network was trained for the best test set until the number of events was more than 20000 for the test set after it had reached to the minimum average error for the test set. The performance of all classifiers was tested by pair-wise, two class, and four class classification methods.

NeuroShell 2 (Ward Systems Group, Inc., Frederick, MD) software was used to develop a neural network model for classification of patterns into several classes. The sample set of 300 kernels was divided into independent training (210 kernels),

test (60 kernels), and validation (30 kernels) sets. The neural network was trained by comparing the input pattern presented to net with the target output. The weights were adjusted according to the learning rule and the difference between target output and network output. In BPNN, errors are always passed backward from output to input in the training. The local minima of error weight function were minimized by random presentation of input patterns to the network in training. The information obtained in training was stored in the interconnections or weights and then applied to the test set. The analysis was repeated for three different training, test, and validation sets for each fungal species and average results were reported.

3.5.4 Classification methods

The classification accuracies of all statistical and neural network classifier were tested by pair-wise, two class, and four class classification methods. In Pair-wise classification, total sample set of 600 kernels (300 healthy kernels + 300 infected kernels) was tested for classification accuracy of healthy kernels vs. each fungal-infected species by all the classifiers. The two class method was performed in two different ways. In case 1, all the fungal damaged samples were grouped into one group (900 kernels) and healthy kernels into the other group (300 kernels) while in case 2, 100 kernels for each fungal species were grouped into one group (300 mixed infected kernels) and healthy kernels into the other group (300 kernels). In the four class classification was performed by grouping each damaged species into independent groups (1, 2, 3) and healthy kernels into another group (4). For all classification methods, each group was divided into 80% training and 20% test samples for statistical classifiers and 70% training, 20% testing, and 10% validation for the neural network.

4. RESULTS AND DISCUSSION

The pair-wise, two-way, and four-way classification methods were used to classify *A. niger, A. glaucus,* and *Penicillium* spp. from healthy wheat kernels. Each sample set of 300 kernels was divided into 80:20 ratio for training (240 kernels) and test set (60 kernels) for statistical classification whereas for artificial neural network each sample set was divided into 70:20:10 for training (210 kernels), test set (60 kernels), and validation (30 kernels). The statistical (linear, quadratic, and Mahalanobis) and back propagation neural network (BPNN) classifiers were tested with 6 statistical and 28 textural features.

4.1 Statistical Classification

4.1.1 Pair-wise classification

The pair-wise classification was carried out to test the potential of the soft X-ray method for identification of healthy and fungal infected kernels (Table 4.1). All classifiers correctly classified all fungal species from healthy wheat kernels with accuracy above 75% (Table 4.1). Linear classifier gave the best classification results for all fungal species and healthy kernels with average accuracies of 91.1 and 89.5%, respectively, whereas quadratic and Mahalanobis classifiers poorly discriminated healthy kernels from *A. niger* with accuracy lower than 80%. Average classification results obtained by the quadratic and Mahalanobis classifiers were lower than the linear classifier. It might be due to the difference between linear and other classifiers in calculating the covariance matrices. Linear classifier applies the same pooled covariance for all classes while quadratic classifier estimates covariance for each class separately.

Table 4.1 Pair-wise classification of healthy and fungal infected wheat kernels by statistical classifiers.

Classifier	Healthy Vs. *A. niger*		Healthy Vs. *A. glaucus*		Healthy Vs. *Penicillium*	
	Healthy (%)	*A. niger* (%)	Healthy (%)	*A. glaucus* (%)	Healthy (%)	*Penicillium* (%)
Linear	90.0	87.2	87.8	90.6	90.6	95.6
Quadratic	77.8	90.0	83.3	86.7	85.0	96.1
Mahalanobis	78.9	86.1	85.6	85.6	93.3	89.4

Table 4.2 Pair-wise classification of fungal infected wheat kernels by statistical classifiers.

Classifier	*A. niger* Vs. *A. glaucus*		*A. niger* Vs. *Penicillium*		*A. glaucus* Vs. *Penicillium*	
	A. niger (%)	*A. glaucus* (%)	*A. niger* (%)	*Penicillium* (%)	*A. glaucus* (%)	*Penicillium* (%)
Linear	68.3	60.0	82.2	88.3	88.9	91.7
Quadratic	67.8	62.2	68.3	88.3	65.0	93.9
Mahalanobis	77.2	43.3	93.3	69.4	81.7	85.0

Also, this method was tested to discriminate between the fungal species (Table 4.2). *Penicillium* spp. was correctly classified from *A. glaucus* with accuracy above 85% by all the classifiers except the quadratic classifier. Mahalanobis classifier correctly classified *A. niger* and *A. glaucus* from *Penicillium* with maximum accuracy (93.3% and 81.7%, respectively) but it failed to differentiate *Penicillium* from *A. niger* (<75%). All classifiers poorly separated *A. glaucus* and *A. niger* by all the classifiers. It might be due to lack of significant difference in density between these two species. Linear classifier gave the best average classification results (79.9%) that might be due to the same reason as stated above.

4.1.2 Two class method

In case 1, all the classifiers detected all types of fungal species with 1-10% misclassifications demonstrating the potential of soft X-rays to separate infected kernels from healthy kernels (Tables 4.3, 4.4). The classification accuracy of linear classifier was better than the rest of the classifiers for healthy kernels in the both cases. In case 1, Mahalanobis classifier gave the best results for all types of fungal species especially for *Penicillium* (98.9%) (Table 4.3). In case 2, the results for all the classifiers were slightly improved for healthy kernels whereas classification accuracy for fungal infected kernels was slightly reduced (Table 4.4). The difference in classification accuracies of healthy and fungal infected kernels in case 1 and case 2 might be due to the number of kernels in sample set. Case 2 has more unbiased distribution of healthy and infected kernels than case 1 as it has equal number of healthy and infected kernels (300 each).

However, this method is not able to differentiate between the infected species. This could be potentially due to lower but similar density in all fungal damaged kernels and thus similar grey-level distribution of the infected kernel images.

Table 4.3 Two class classification of wheat kernels by various statistical classifiers (Case 1: 300 healthy and 900 all infected kernels).

	Healthy (%)	*A. niger* (%)	*A. glaucus* (%)	*Penicillium* (%)
Linear	82.8	89.4	91.1	92.8
Quadratic	73.9	90.0	91.1	97.2
Mahalanobis	71.7	92.2	92.2	98.9

Table 4.4 Two class classification of wheat kernels by various statistical classifiers (Case 2: 300 healthy and 300 mixed infected kernels equal for each species).

	Healthy %	Infected kernels %
Linear	86.7	86.1
Quadratic	76.1	86.6
Mahalanobis	78.3	84.4

4.1.3 Four class method

In four class method, very poor classification results were obtained by all classifiers with exception of linear and quadratic classifiers, which correctly classified *Penicillium* samples with accuracy more than 85% (Tables 4.5, 4.6, 4.7). All the classifiers highly misclassified *A. glaucus* and *A. niger* with each other which might be due to the same reason discussed above. Also, this method gave poor results for healthy kernels.

Table 4.5 Four class classification of wheat kernels by linear statistical classifier.

	Healthy (%)	***A. niger* (%)**	***A. glaucus* (%)**	***Penicillium* (%)**
Healthy	**74.4**	5.0	10.0	10.6
A. niger	7.8	**57.2**	27.2	7. 8
A. glaucus	5.6	26.1	**60.0**	7. 2
Penicillium	2.2	6.7	5.6	**85. 6**

Table 4.6 Four class classification of wheat kernels by quadratic statistical classifier.

	Healthy (%)	*A. niger* (%)	*A. glaucus* (%)	*Penicillium* (%)
Healthy	**69.4**	15.6	7.8	7.2
A. niger	6.7	**51.7**	21.1	20.6
A. glaucus	5.6	22.2	**50.6**	21.7
Penicillium	1.1	8.3	4.4	**86.1**

Table 4.7 Four class classification of wheat kernels by Mahalanobis statistical classifier.

	Healthy (%)	*A. niger* (%)	*A. glaucus* (%)	*Penicillium* (%)
Healthy	**75.0**	17.8	6.7	0.6
A. niger	9.4	**68.3**	17.8	4.4
A. glaucus	5.6	33.9	**47.8**	12.8
Penicillium	5.6	23.3	4.4	**67.2**

4.2 Artificial Neural Network

4.2.1 Pair-wise classification

In pair-wise method, BPNN classifier discriminated fungal infected kernels from healthy kernels correctly with 80 to 94.6 % classification accuracy for training, testing and validation sets (Table 4.8). Training set of *Penicillium* spp. infected kernels attained the maximum accuracy of 94.6% whereas testing set of *A. niger* had the lowest classification accuracy of 80%. Validation sets had almost the same accuracy for *A. niger* (87.8%), *A. glaucus* (86.7%), and *Penicillium* spp. (88.9%). Average classification accuracies of training, testing and validation sets of healthy kernels were 89.1, 84.6, and 90.4%, respectively.

Back-propagation neural network classifier was also tested for classification within fungal infected species by the pair-wise method (Table 4.9). *Penicillium* spp. was classified from *A. glaucus* with the highest classification accuracy in training (88.7%), testing (85.6%), and validation set (92.2%). *A. niger* and *A. glaucus* were highly misclassified with each other in training, testing and validation sets and hence attained comparatively poor classification accuracy (<80%). *A. glaucus* was discriminated from *Penicillium* spp. with accuracy >83.3% while *A. niger* and *Penicillium* spp. were discriminated with 80 to 88.9% accuracy in all the sets.

Table 4.8 Pair-wise classification of healthy and fungal infected wheat kernels by BPNN classifiers.

	Healthy Vs *A. niger*		Healthy Vs. *A. glaucus*		Healthy Vs. *Penicillium*	
	Healthy %	*A. niger* %	Healthy %	*A. glaucus* %	Healthy %	*Penicillium* %
Training	90.0	86.8	87.8	89.5	89.4	94.6
Testing	83.3	80.0	82.2	83.9	88.3	88.9
Validation	90.0	87.8	90.0	86.7	91.1	88.9

Table 4.9 Pair-wise classification of fungal infected wheat kernels by BPNN classifiers.

	A. niger Vs. *A. glaucus*		*A. niger* Vs. *Penicillium*		*A. glaucus* Vs. *Penicillium*	
	A. niger %	*A. glaucus* %	*A. niger* %	*Penicillium* %	*A. glaucus* %	*Penicillium* %
Training	70.5	62.2	85.7	86.8	88.4	88.7
Testing	68.3	58.9	81.1	82.8	83.3	85.6
Validation	76.7	63.3	88.9	80.0	86.7	92.2

4.2.2 Two class classification

In case 1, two class method discriminated *A. niger*, *A. glaucus*, and *Penicillium* spp. with accuracy >90% (Table 4.10). The maximum accuracy was attained for the validation set of *Penicillium* sample (97.8%) preceded by training set of *A. glaucus* (96%) whereas BPNN classifier was unable to identify healthy kernels by this method (<75%). Test set of *A. niger* and *Penicillium* spp. had accuracy of 95.6% while test set of *A. glaucus* and training set of *A. niger* were identified with accuracy of about 94%. Validation sets of *A. niger* and *A. glaucus* attained 92.2% accuracy. In case 2, the classification accuracy for healthy kernels was improved tremendously (92.2%) whereas accuracy for fungal infected kernels was reduced to 84.4% in validation set (Table 4.11). The increase in classification accuracies of healthy kernels could be due to unbiased distribution of healthy and infected kernels (300 kernels each) in training set.

4.2.3 Four class classification

Training set of *Penicillium* spp. was correctly identified by BPNN classifier with four class classification method with maximum accuracy of 91.3% (Table 4.12). This method poorly classified healthy, *A. niger*, and *A. glaucus* (<75%).

Table 4.10 Two class classification of wheat kernels by BPNN classifiers (Case 1: 300 healthy and 900 all infected kernels).

	Healthy %	*A. niger* %	*A. glaucus* %	*Penicillium* %
Training	62.7	93.8	96.0	95.9
Testing	57.8	95.6	93.9	95.6
Validation	60.0	92.2	92.2	97.8

Table 4.11 Two class classification of wheat kernels by BPNN classifiers (Case 2: 300 healthy and 300 mixed infected kernels equal for each species).

	Healthy %	Fungal Infected kernels %
Training	87.5	83.2
Testing	80.6	82.2
Validation	92.2	84.4

Table 4.12 Four class classification of wheat kernels by BPNN classifiers.

	Healthy %	*A. niger* %	*A. glaucus* %	*Penicillium* %
Training	62.7	20.6	44.8	91.3
Testing	53.9	17.8	43.3	84.4
Validation	58.9	12.2	51.1	88.9

Pearson et al. (2006) reported accuracy of 82.5% for visible spectra while Walcott et al. (1998) used ultrasound signals to detect the level of fungal infection with r^2 =0.85. Also, transmittance and reflectance spectra can detect 81 to 98% fungal infection (Pearson et al., 2001; Delwiche, 2003; Pearson et al., 2004; Wang et al., 2004; Pearson et al., 2006). Pearson et al (2006) stated classification accuracy of 82% for fungal infected maize kernels and 100% for healthy kernels for soft X-ray method. In the present study, all classifiers could classify healthy kernels with accuracy >85% by the pair-wise method. Fungal infected kernels were discriminated from healthy kernels with the 80 to 98.9% accuracy by statistical and neural network classifiers with pair-wise and two class methods whereas the four class method was unable to classify healthy and infected kernels with good accuracy. Linear classifier gave better results for healthy kernels (82.8%) than neural network classifier (<75%) by the two class method.

5. CONCLUSION

The soft X-ray method has the potential to detect fungal infection by A. *niger*, A. *glaucus*, and *Penicillium* spp in stored wheat. This method can differentiate healthy and infected kernels by linear statistical classifier and neural network classifier with accuracy >85%.

In pair-wise method, linear statistical classifier classified 87 to 95% infected and 87 to 90% healthy kernels. Quadratic and Mahalanobis classifiers detected 83.3 to 96.1% infected kernels but highly misclassified healthy kernels with *A. niger.* Neural network classifier detected healthy kernels with accuracy >90% and infected kernels with accuracy 86.7 to 88.9%. Whereas all the classifiers misclassified *A. niger* and *A. glaucus* infected kernels.

In two class method (Case 1: 300 healthy and 900 all infected kernels), quadratic and Mahalanobis classifier classified 90.0 to 98.9% infected kernels but gave high false positive error (26.1 and 28.3%, respectively). Linear classifier classified 82.8% healthy kernels but only detected 89.4 to 92.8% infected kernels. Neural network classifier detected 92.2 to 97.8% infected kernels but gave very high false positive (40%).

In two class method (Case 2: 300 healthy and 300 mixed infected kernels equal for each species), linear classifier discriminated healthy and infected kernels with 86.7 and 86.1%. The quadratic and Mahalanobis classifiers detected infected kernels with accuracy 86.6 and 84.4%, respectively but highly misclassified healthy kernels

(<80%). Neural network classifier detected 92.2% healthy kernels and 84.4% infected kernels.

In four class method, all the classifiers poorly classified healthy and fungal infected kernels.

6. REFERENCES

Abbott, J.A. 1999. Quality measurement of fruits and vegetables. *Postharvest Biology and Technology* 15:207-225.

Anonymous. 2007. Topic 7 X-Rays. http://www.antonine-education.co.uk /Physics_A2/ Options/Module_6/Topic_7/topic_7_x.htm (2007-04-07)

Arnheim N. and H. Erlich. 1992. Polymerase chain reaction strategy. *Annual Review of Biochemistry* 61:131-56.

Assante G., L. Camarda, R. Locci, L. Merlini, G. Nasini, and E. Papadopoules. 1981. Isolation and structure of red pigments from *Aspergillus flavus* and related species, grown on differential medium. *Journal of Agricultural Food Chemistry* 29:785-787.

Attwood, D. 1999. *Soft X-rays and Extreme Ultraviolet Radiation-Principles and Applications.* New York, NY: Cambridge University Press.

Baldo, B.A., P.A. Boniface, and D.H. Simmonds. 1982. Lectins as Cytochemical probes of the developing wheat grain. II. Reaction of wheat-germ lectin with the nucellar epidermis. *Australian Journal of Plant Physiology* 9:663-675.

Banks, J. and P. Fields. 1995. Physical methods for insect control in stored grain ecosystems. In *Stored-Grain Ecosystems*, eds. D.S. Jayas, N.D.G. White and W.E. Muir, 353-409. New York, NY:Marcel Dekker, Inc.

Barcelon, E.G., S. Tojo, and K. Watanabe. 1999. X-ray CT imaging and quality detection of peach at different physiological maturity. *Transaction of the ASAE* 42:435-441.

Barker D.A., T.A. Vuori, M.R. Hegedus, and D.G. Myers. 1992. The use of ray parameters for the discrimination of Australian wheat varieties. *Plant Varieties and Seeds* 5:35-45.

Belcher, E.W. 1968. Use of soft X-rays in tree seed testing and research. In *Proceedings of Southeastern Forest Radiography Workshop*, 74-96. University of Georgia, Athens, GA. cited by Schnurer et al. (1999).

Borjesson, T. 1993. *Volatile Fungal Metabolites as Indicators of Mould Growth in Stored Cereals.* Unpublished Ph.D. thesis. Swedish University of Agricultural Sciences, Uppsala cited by Schnurer et al. (1999).

Borjesson, T., U. Stollman, and J. Schnurer. 1993. Off-odorous compounds produced by moulds on oatmeal agar: Identification and relations to other growth characteristics. *Journal of Agricultural Food Chemistry* 41:2104–2111.

Bothast R.J. and D.I Fennel. 1974. A medium for rapid identification and enumeration of *Aspergillus* and related organisms. *Mycologia* 66:365-369.

Bowers, S.V., III. 1989. Nondestructive testing to determine the internal quality of peaches. Unpublished Ph.D. thesis. Clemson University, Clemson, SC. Cited by Han et al. (1992).

Brecht, J.K., R.L. Shewfelt, J.C. Garner, and E.W. Tollner. 1991. Using X-ray computed tomography to non-destructively determine maturity of green tomatoes. *Hortscience* 26(1):45-47.

Brodsky, M.H., P. Entis, M.P. Entis, A. Sharpe, and G.A. Jarvis. 1982. Determination of aerobic plate and yeast and mould counts in foods using an automated

hydrophobic grid membrane filter technique. *Journal of Food Protection* 45:301-304.

Bullerman, L.B. and D.I. West. 1990. Comparison of several media and methods for detecting and enumeration toxigenic *Fusarium* species. In *Proceedings Standard methods of mycological examination of foods*, 25-26 Baarn, The Neatherlands.

Chen, Z., Y. Tao, H. Jing, and J. Walker. 2001. Internal inspection of deboned poultry using X-ray imaging and adaptive thresholding. *Transactions of the ASAE* 44(4):1005–1009.

Christensen, C. M. and R. A. Meronuck. 1988. Dry matter loss in yellow dent corn resulting from invasion by storage fungi. *Plant Disease* 73:501-503.

Council for Agricultural Science and Technology. 1989. Mycotoxins: Economic and Health risks. Report 116. CAST, Ames, Iowa.

Curry T.S., J.E. Dowdey, and R.C. Murry Jr. 1990. *Christensen's Physics of Diagnostic Radiology*, 4th ed. Malvern, PA: Lea and Febiger Ltd.

Dakers, S. and J. D Frechette. 1998. The relative position of Canada in the world grain market. http://dsp-psd.pwgsc.gc.ca/Collection-R/LoPBdP/modules/prb98-2-grain/grainmarket-e.htm (2008-04-20).

Delwiche, S. R. 2003. Classification of scab and other mold-damaged wheat kernels by near-infrared reflectance spectroscopy. *Transactions of the ASAE* 46(3): 731-738.

Dewey, F.M., D.R. Twiddy, S.I. Phillips, M.J. Grose, and P.W. Wareing. 1992. Development of a quantitative monoclonal antibody-based immunoassay for *Humicola lanuginosa* on rice grains and comparison with conventional assays. *Food and Agricultural Immunology* 4:153-67.

Farber, P., R. Geisen, and W.H. Holzapfel. 1997. Detection of aflatoxinogenic fungi in figs by a PCR reaction. *International Journal of Food Microbiology* 36:215-220.

Fenton, F.A. and W.W. Waite. 1932. Detecting pink Bollworms in cottonseeds by the X-ray. *Journal of Agricultural Engineering Research* 45(6):347-348.

Fiedler, J.C., B.G. Wilkinson, K.L. Edney, and R.O. Sharples. 1973. The biology of apple and pear storage. Research Review No. 3. East Malling, England: Commonwealth Bureau of Horticulture and Plantation Crops, Commonwealth Agriculture Bureau cited by Kim et al. (2000).

Finney, E.E. and K.H. Norris. 1978. X-ray scans for detecting hollow heart in potatoes. *American Potato Journal* 55:95-105.

Flannigan, B. and M.S.O. Bana. 1980. Growth and enzyme production in *Aspergilli* which cause biodeterioration in stored grain. *Cereal Chemistry* 62:137-44.

Fornal, J., T. Jelinski, J. Sadowska, S. Grundas, J. Nawrot, A. Niewiada, J.R. Warchalewski and W. Blaszczak. 2007. Detection of granary weevil *Sitophilus granarius* (L.) eggs and internal stages in wheat grain using soft X-ray and image analysis. *Journal of Stored Products Research* 43:142-148.

Gaunt, D.M., A.P.J. Trinci, and J.M. Lynch. 1985. The determination of fungal biomass using adenosine triphosphate. *Experimental Mycology* 9:174-178.

Ghosh, J. and B. Nandi. 1986. Deteriorative abilities of some common storage fungi of wheat. *Seed Science and Technology* 14:141-149.

Gonzaleze, R.C. and R.E. Woods. 1998. *Digital Image Processing*. New York, NY: Addison-Wesley.

Gourama, H. and L.B. Bullerman. 1995. Detection of moulds in foods and feeds: potential rapid and selective methods. *Journal of Food Protection* 58(12):1389-1394.

Grainaissance Inc. 1999. What is Amazake? http://www.grainaissance.com /amazake.ht ml (2007/08/16).

Gurney, K. 1997. *An Introduction to Neural Network.* 1st ed. London: UCL Press Ltd.

Haff, R.P. and D.C. Slaughter. 2002. X-ray inspection of wheat for granary weevils. real-time digital imaging vs. film. ASAE Paper No. 026093. St. Joseph, MI: ASAE.

Haff, R.P. and D.C. Slaughter. 2004. Real-time X-ray inspection of wheat for infection by the Granary weevil, *Sitophilus Granarius* (L.). *Transactions of the ASAE* 47(2):531-537.

Han, Y.J., S.V., Bowers, III, and R.B. Dodd. 1992. Non-destructive detection of split pit peaches. *Transactions of the ASAE* 35 (6):2063-2067.

Haskins, C. P. and C. N. Moore. 1935. Growth modifications in citrus seedlings grown from X-rayed seed. *Plant Physiology* 10:179-85.

Hastings, J.W., W.Y.J. Tsai, and L.B. Bullerman. 1984. Comparison of plate-MPN technique with plate surface count for mould enumeration. In *Methods for the Mycological Examinations of the Foods*, eds., A.D. King, J.I. Pitt, L.R. Beuchat, and J.E.L. Corry, NATO ASI Series, New York, NY: Plenum Press.

Hooker, D. 2007. Back to the womb and out again with Dogash. http://www.dogash.com/chap001.htm. (2008/06/15).

Hornok, L. and A. Jagicza 1973. Fluorescent antibody staining of Fusarium culmorum. *Acta Phytopathologica Academiae Scientiarum Hungaricae* 8:357-63.

International Commission on Radiological Protection. 1990. *Recommendations of the International Commission on Radiological Protection.* Oxford: Pergamon Press; ICRP Publications 60; 1991.

Jain, P.C., J. Lacey, and L. Stevens. 1991. Use of API-Zym strips and 4-nitrophenyl substrates to detect and quantify hydrolytic enzymes in media and grain colonised with *Aspergillus*, *Eurotium*, and *Penicillium* spp. *Mycological Research* 95:834-842.

Jarvis, B., D.A.L. Sciler, A.J.L. Ould, and A.P. Williams. 1983. Observations on the enumeration of molds in food and feedstuffs. *Journal of Applied Bacteriology* 55:325.

Jayas, D.S., J. Paliwal, and N.S. Visen. 2000. Multi-layer neural networks for image analysis of agricultural products. *Journal of Agricultural Engineering Research* 77(2):119-128.

Jerkins, R. and D.J. Haas. 1973. Hazards in the use of X-ray analytical instrumentation. *X-Ray Spectrometry* 2(3):135-141.

Kamphuis, H.J., S. Notermans, G.H. Veeneman, J.H. van Boom, and F.M. Rombouts. 1989. A rapid and reliable method for the detection of moulds in foods: using latex agglutination assay. *Journal of Food Protection* 52:244-247.

Karunakaran C., J. Paliwal, D. S. Jayas, and N. D. G. White. 2005. Comparison of soft X-rays and NIR spectroscopy to detect insect infections in grain. ASAE Paper No. 053139. St. Joseph, Mich.:ASAE.

Karunakaran, C., D. S. Jayas and N.D.G. White. 2004a. Detection of internal wheat seed infection by *Rhyzopertha dominica* using X-ray imaging. *Journal of Stored Products Research* 40:507-516.

Karunakaran, C., D.S. Jayas, and N.D.G. White. 2004b. Identification of wheat kernels damaged by the red flour beetle using X-ray images. *Biosystems Engineering* 87(3):267-274.

Keagy, P.M. and T.F. Schatzki. 1991. Effect of image resolution on insect detection in wheat radiograms. *Cereal Chemistry* 68(4):339-343.

Keagy, P.M. and T.F. Schatzki. 1993. Machine recognition of weevil damage in wheat radiographs. *Cereal Chemistry* 70(6):696-700.

Kim, S and T.F. Schatzki. 2000. Apple watercore sorting system using x-ray imagery: I. Algorithm development. *Transactions of the ASAE* 43(6):1695-1702.

Kumar, P.A. and S. Bal. 2007. Automatic unhulled rice grain crack detection by X-ray imaging. *Transactions of ASABE* 50(5):1907-1911.

Kylafis, N. 2005. Spectra and temporal variability of galactic black-hole X-ray sources in the hard state. www.astro.lsa.umich.edu/Events/Meetings/mctp (2007/08/26).

Larsen, T. O. 1997. Identification of cheese-associated fungi using selected ion-monitoring of volatile terpenes. *Letters in Applied Microbiology* 24:463–466 cited by Schnurer et al. (1999).

Lenker, D.H. and P.A. Adrian. 1971. Use of X-rays for selecting mature lettuce heads. *Transactions of the ASAE* 14(5):894-898.

Lin H.H. and M.A. Cousin. 1985. Detection of mould in processed food by high performance liquid chromatography. *Journal of Food Protection* 48:671-678.

Luo, X.Y., D.S. Jayas, and S.J. Symons. 1999. Identification of damaged kernels in wheat using a colour machine vision system. *Journal of Cereal Science* 30:49-59.

Magan, R. 1993. Early detection of fungi in stored grain. *International Biodeterioration and Biodegradation* 32:145-160.

Majumdar S. and D.S. Jayas. 2000. Classification of cereal grains using machine vision: iii. texture models. *Transactions of ASAE* 43(6): 1681-1687.

Manonmani, H.K., S. Anand, A. Chandrashekar, and E.R. Rati. 2005. Detection of aflatoxigenic fungi in selected food commodities by PCR. *Process Biochemistry* 40:2859-2864.

Matrai, T., S. Mayer, S. Kokai, and I. Salamon. 2000. Invertase production of common storage moulds in food and feed grains as a possibility for rapid detection of *Aspergillus flavus* group and *Aspergillus fumigatus*. *International Journal of Food Microbiology* 61:187–191.

Mills, R.B. and D.A. Wilbur. 1967. Radiographic studies of Angoumois grain moth development in wheat, corn and sorghum kernels. *Journal of Economic Entomology* 92(2):453-462.

Milner, M., M.R. Lee and R. Katz. 1950. Application of X-ray technique to the detection of internal insect infection of grain. *Journal of Economic Entomology* 43(6):933-935.

Milner, M., M.R. Lee and R. Katz. 1952. Radiography applied to grain and seeds. *Food Technology* 6:44-45.

Mitchell, T.M. 2006. Learning Classifiers based on Bayes Rule. http://www.cs.cmu.edu/~tom/mlbook/NBayesLogReg.pdf (2007/09/23).

Monash University. 2003. Synchrotron strategy group. www.vcp.monash.edu.au/research /synchrotron.html (2007/09/23).

Murray, I. and P.C. Williams. 1990. Chemical principles of near-infrared technology. 1990. In: *Near-infrared Technology in the Agricultural and Food Industries*, eds. P. Williams and K. Norris, St. Paul, MN: American Association of Cereal Chemists.

Myers, D.G. and K.J. Edsall. 1989. The application of image processing techniques to the identification of Australian wheat varieties. *Plant Varieties and Seeds* 2:109-116.

Neethirajan, S. and D. S. Jayas. 2006a. Network analysis of grain bulk pore structure using high resolution X-ray computed tomography images. CSBE/SCAEB Paper No. 06-122, Winnipeg, MB:CSBE.

Neethirajan, S., C. Karunakaran, D.S. Jayas, and N.D.G. White. 2004. X-ray CT image analysis to determine air flow path in grain bulks. ASAE/CSAE Paper No. 043080, St. Joseph, MI:ASAE.

Neethirajan, S., D.S. Jayas, and N.D.G. White. 2007a. Detection of sprouted wheat kernels using soft X-ray image analysis. *Journal of Food Engineering* 81:509-513.

Neethirajan, S., D.S. Jayas, and C. Karunakaran. 2007b. Dual energy X-ray image analysis for classifying vitreousness in durum wheat. *Postharvest Biology and Technology* 45:381-384.

Neethirajan,S., C. Karunakaran, S. Symons, and D.S. Jayas. 2006b. Classification of vitreousness of Durum wheat using soft X-rays and transmitted light images. *Computer and Electronics in Agriculture* 53:71-78.

Newell, S.Y. 1992. Estimating fungal biomass and productivity in decomposing litter. In *The Fungal Community-Its Organisation and Role in the Ecosystem*, eds. G. C. Carroll and D.T.Wicklow, 2nd ed., 521–561. New York, NY: Marcel Dekker.

Notermans, S. and C.J. Heuvelman. 1985. Immunological detection of moulds in food by using the enzyme linked immunosorbent assay (ELISA); preparation of antigens. *International Journal of Food Microbiology* 2:247-248.

Notermans, S. and H.J. Kamphuis. 1992. Detection of fungi in foods by latex agglutination: a collaborative study. In *Modern Methods of Food Mycology*, eds. R.A. Samson, A.D. Hocking, J.I. Pitt, and A.D. King, 205-212. New York, NY: Elsevier.

Notermans, S., C.J. Heuvelman, R.R. Beumer, and R. Maas. 1986. Immunological detection of moulds in foods relation between antigen production and growth. *International Journal of Food Microbiology* 3:253-261.

Oblinger, J.L. and J.A. Koburger. 1975. Understanding and teaching the most probable number technique. *Journal of Milk Food Technology* 38(9):540-545.

Ogawa, Y., K. Morita, S. Tanaka, M. Setoguchi, and C.N. Thai. 1998. Application of X-ray CT for detection of physical foreign materials in food. *Transactions of the ASAE* 41(1):157-162.

Ordaz, J. J., C.A. Fente, B.I. Vazquez, C.M. Franco, and A. Cepeda. 2003. Development of a method for direct visual determination of aflatoxin production by colonies of the *Aspergillus flavus* group. *International Journal of Food Microbiology* 83:219-225.

Paliwal J., N.S. Shashidhar, and D.S. Jayas. 1999. Grain kernel identification using kernel signature. *Transactions of ASAE* 42(6):1921-1924.

Paliwal, J., N.S. Visen, D.S. Jayas, and N.D.G. White. 2005. Quantification of variations in Machine-vision-computed morphological features of cereal grains. *Canadian Biosystems Engineering* 47:7.1-7.6.

Patel, V.C., R.W. McClendon, and J.W. Goodrum. 1996. Detection of blood spots and dirt stains in eggs using computer vision and neural networks. *Applied Engineering in Agriculture* 12(2):253-258.

Pavlidis, T. 1980. Algorithms of shape analysis of contours and waveforms. *IEEE Transactions on Pattern Analysis and Machine Intelligence* 2(4):301-312.

Payne, G.E., G.J. Nystrum, B. Bhatnagar, T.E. Cleveland, and C.P. Woloshuk. 1993. Cloning of the afl-2 gene involved in aflatoxin biosynthesis from *Aspergillus flavus*. *Applied Environmental Microbiology* 59:156-162.

Pearson, T.C. and D.T. Wicklow. 2006. Detection of kernels infected by fungi. *Transactions of the ASABE* 49(4):1235-1245.

Pearson, T.C., D.T. Wicklow, and M.C. Pasikatan. 2004. Reduction of aflatoxin and fumonosin contamination in yellow corn by high speed duel wave-length sorting. *Cereal Chemistry* 81(4):490-498.

Pearson, T.C., D.T. Wicklow, E.B. Maghirang, F. Xie, and F.E. Dowell. 2001. Detecting aflatoxin in single corn kernels by using transmittance and reflectance spectroscopy. *Transactions of the ASAE* 44(5):1247-1254.

Pedersen, J.R. and R.A. Brown. 1960. X-ray microscope to study behavior of internal infecting grain insects. *Journal of Economic Entomology* 53:678-679.

Pitt, J.I. 1990. Collabrative study on media for the detection and differentiation of *Aspergillus flavus* and *A. parasiticus* and the detection of aflatoxin production. In *Proceedings Standard Methods of Mycological Examination of Foods,* 28. Baarn, the Neatherlands.

Pitt, J.I., A.D. Hocking, and D.P. Glenn. 1983. An improved medium for the detection of *Aspergillus flavus* and *A. Parasiticus*. *Journal of Applied Bacteriology* 54:109-114.

Prescott J.M., P.A. Burnett, E.E. Saari, J. Ranson, J. Bowman, W. de Milliano, R.P. Singh, and G. Bekele. 2007. Wheat diseases and pests: a guide for field identification. http://wheat.pw.usda.gov/ggpages/wheatpests.html#karnalb unt (2007/8/16).

Rao S.B., V.S. Rao, Y. Ramakrishna, and R.V. Bhat. 1989. Rapid and specific method for screening ergosterol as an index of fungal contamination in cereal grains. *Food Chemistry* 31:51-56.

Rex, B.L. and G. Mazza. 1989. Cause, control and detection of hollow heart in potatoes: *American Potato Journal* 66:165-183.

Richards, J.A., F.W. Sears, M.R. Wehr, and M.W. Zemansky. 1960. *Modern university physics,* London, UK: Addison-Wesley.

Ride J.P. and R.B. Drysdale. 1972. A rapid method for the chemical estimation of filamentous fungi in plant tissue. *Physiology and Plant Pathology* 2:7-15.

Robertson, J.C. 1976. *A Guide to Radiation Protection,* New York, NY:John Wiley and Sons, Inc.

Samson, R.A., E.S. Hoekstra, J.C. Frisvad, and O. Filtenborg. 1996. *Introduction to Food-Borne Fungi,* 5th edition. Centraal-bureau voor Schimmelcultures, Baarn and Delft. Cited by Schnurer et al. (1999).

Sashidhar R.B., R.V. Sudershan, Y. Ramkrishna, S. Nahdi, and R.V. Bhat. 1988. Enhanced fluorescence of ergosterol by iodination and determination of ergosterol by fluorodensitometry. *Analyst* 113(5):809-812.

Schatzki, T.F. and T.A. Fine. 1988. Analysis of radiograms of wheat kernels for quality control. *Cereal Chemistry* 65(3):233-239.

Schatzki, T.F., R.P. Haff, R. Young, I. Can, L.C. Le, and N. Toyofuku. 1997. Defect detection in apples by means of X-ray imaging. *Transaction of the ASAE* 40: 1407-1415.

Schnurer, J., J. Olsson, and T. Borjesson.1999. Fungal volatiles as indicators of food and feeds spoilage. *Fungal Genetics and Biology* 27:209-217.

Scotter, J.M., V.C. Langford, F.P. Wilson, M.J. McEwan, and S.T. Chambers. 2005. Real-time detection of common microbial volatile organic compounds from medically important fungi by selected ion flow tube-mass spectrometry (SIFT-MS). *Journal of Microbiological Methods* 63:127-134.

Seitz, L.M., D.B. Sauer, R. Burroughs, H.E. Mohr, and J.D. Hubard. 1979. Ergosterol as a measure of fungal growth. *Phytopathology* 69:1202-1203.

Seitz, L.M., H.E. Mohr, R. Burroughs, and D.B. Sauer. 1977. Ergosterol as an indicator of fungal invasion in grains. *Cereal Chemistry* 54:1207-1217.

Seitz. L.M., D.B. Saucer, H.E. Mohr, and R. Burroughs. 1975. Weathered grain sorghum: Natural occurrence of alternariols and storability of the grain. *Phytopathology* 65:1259-1263.

Sellars, P.N., C.E.C. McGill, and B. Flannigan. 1976. Degradation of barley by *Aspergillus fumigatus* Fres. In *Proceedings of the 3rd International Biodeterioration Symposium,* eds. J.M. Sharpley and A.M. Kaplan. Applied Science Publishers, 633-643. London.

Shahin, M.A. and E.W. Tollner. 1997. Apple classification based on watercore features using fuzzy logic. ASAE Paper No. 97-3077. St. Joseph, MI: ASAE.

Shahin, M.A. E.W. Tollner, R.D. Gitaitis, D.R. Sumner, and B.W. Maw. 2002. Classification of sweet onions based on internal defects using image processing and neural network techniques. *Transactions of the ASAE* 45(5):1613-1618.

Shahin, M.A., E.W. Tollner, M.D. Evans, and H.R. Arabnia. 1999. Watercore features for sorting red delicious apples: A statistical approach. *Transactions of the ASAE* 42(6): 1889-1896.

Sharifi, S. and R.B. Mills. 1971a. Radiographic studies of *Sitophilus Zeamais* in wheat kernels. *Journal of Stored Products Research* 7(3):195-206.

Sharifi, S. and R.B. Mills. 1971b. Developmental activities and behavior of the rice weevil inside wheat kernels. *Journal of Economic Entomology* 64(5):1114-1118.

Singh, C.B., D.S. Jayas, J. Paliwal, and N.D.G. White. 2007. Fungal detection in wheat using near-infrared hyper-spectral imaging. *Transactions of the ASABE*. 50(6):2171-2176.

Sonego, L., R. Ben-Arie, J. Raynal, and J.C. Pech. 1995. Biochemical and physical evaluation of textural characteristics of nectarines exhibiting woolly

breakdown: NMR imaging, X-ray computed tomography and pectin composition. *Postharvest Biology and Technology* 5:187-198.

Stermer, R.A. 1972. Automated X-ray inspection of grain for insect infection. *Transactions of the ASAE* 15(6):1081-1085.

Sukurai, Y. and H. Shiota. 1977. On the convenient method for glucosamine estimation in Koji. *Agricultural and Biological Chemistry* 41:619-624.

The Columbia Electronic Encyclopedia. 2007. http://www.infoplease.com/ce6/sci/A0862028.html (2007/06/30).

Thomas, P., S.C. Saxena, R. Chandra, R. Rao, and C.R. bhatia. 1993. X-ray imaging for detecting spongy tissue, an internal disorder in fruits of 'Alphonso' mango (*Mangifera indica* L.). *Journal of Horticultural Science* 68(5):803-806.

Tollner, E.W. 1993. X-ray technology for detecting physical quality attributes in agricultural produce. *Postharvest News and Information* 4(6):149N-155N.

Tollner, E.W., Y.C. Hung, B. Maw, D.R. Sumner, and R.D. Gitaitis. 1995. Non-destructive testing for identifying poor quality onions. *Proceedings of SPIE Technology Conference* 23(45):392–402 cited by Shahin et al. (2002).

Tollner, E.W., Y.C. Hung, B.L. Upchurch, and S.E. Prussia. 1992. Relating X-ray absorption to density and water content in apples. *Transactions of the ASAE* 35:1921-1928.

USDA. 2008. Grain: World markets and trade. http://www.fas.usda.gov/grain/circular/2008/01-08/grainfull01-08.pdf (2008-04-03).

Walcott, R.R., D.C. McGee, and M.K. Misra. 1998. Detection of asymptomatic fungal infections of soybean seeds by ultrasound analysis. *Plant Disease* 82(5):584-589.

Wang, D., F.E., Dowell, M.S. Ram, and W.T. Schapaugh. 2004. Classification of fungal-damaged soybean seeds using near-infrared spectroscopy. *International Journal of Food Properties* 7(1):75–82.

Warncock, D.W. 1973. Use of immunofluorescence to detect mycelium of *Alternaria*, *Aspergillus*, and *Penicillium* in barley grains. *Transactions of the British Mycological Society* 61:547-52.

Weete, J.D. 1980. *Lipid biochemistry of fungi and other organisms*, New York, NY: Plenum press.

White, P.L., A.E. Archer, and R.A. Barnes. 2005. Comparison of non-culture-based methods for detection of systemic fungal infections, with an emphasis on invasive Candida infections. *Journal of Clinical Microbiology* 43(5):2181-2187.

Wiese, M.V. 1991. *Compendium of Wheat Diseases*, 2nd edition. St. Paul, MN: APS Press.

Wikimedia Foundation Inc. 2007a. Electromagnetic radiation. http://en.wikipedia.org/wiki/Electromagnetic_radiation.html (2007/08/26).

Wikimedia Foundation Inc. 2007b. X-ray. http://en.wikipedia.org/wiki/X-ray.html (2007/06/30).

Wikimedia Foundation Inc. 2007c. Artificial neural network. http://en.wikipedia.org/wiki/Artificial_neural_network (2007/06/30).

Williams, A.P. and J.M. Wood. 1986. Impedimetric estimation of moulds. In *Methods of Mycological Examination of Foods,* eds. A.D. King, J.I. Pitt, L.R. Beuchat, and J.E.L. Corry. New York. NY: Plenum press.

Wort, D.J. 1941. X-ray effects on the growth and reproduction of wheat. *Plant Physiology* 18:373-383.

Yong, R.K. and M.A. Cousin. 2001. Detection of moulds producing aflatoxins in maize and peanuts by an immunoassay. *International Journal of Food Microbiology* 65:27–38.

Zeringue, H. J., D. Bhatnagar, and T.E. Cleveland. 1993. C15H24 volatile compounds unique to aflatoxigenic strains of *Aspergillus flavus. Applied Environmental Microbiology* 59:2264–2270.

Appendix 1

Pair-wise classification of healthy and fungal infected wheat kernels by statistical classifiers

	Healthy Vs. *A. niger*		Healthy Vs. *A. glaucus*		Healthy Vs. *Penicillium*	
	Healthy (%)	*A. niger* (%)	Healthy (%)	*A. glaucus* (%)	Healthy (%)	*Penicillium* (%)
Linear						
Set 1	93.3	88.3	86.7	88.3	91.7	86.7
Set 2	83.3	86.7	88.3	95.0	90.0	100.0
Set 3	93.3	86.7	88.3	88.3	90.0	100.0
Mean	**90.0**	**87.2**	**87.8**	**90.6**	**90.6**	**95.6**
Quadratic						
Set 1	80.0	86.7	73.3	88.3	83.3	88.3
Set 2	73.3	91.7	88.3	83.3	90.0	100.0
Set 3	80.0	91.7	88.3	88.3	81.7	100.0
Mean	**77.8**	**90.0**	**83.3**	**86.7**	**85.0**	**96.1**
Mahalanobis						
Set 1	80.0	85.0	76.7	86.7	93.3	81.7
Set 2	76.7	86.7	90.0	83.3	96.7	91.7
Set 3	80.0	86.7	90.0	86.7	90.0	95.0
Mean	**78.8**	**86.1**	**85.6**	**85.6**	**93.3**	**89.4**

Appendix 2

Pair-wise classification of fungal infected wheat kernels by statistical classifiers

	A. niger Vs. *A. glaucus*		*A. niger* Vs. *Penicillium*		*A. glaucus* Vs. *Penicillium*	
	A. niger (%)	*A. glaucus* (%)	*A. niger* (%)	*Penicillium* (%)	*A. glaucus* (%)	*Penicillium* (%)
Linear						
Set 1	73.3	66.7	75.0	96.7	95.0	100.0
Set 2	65.0	56.7	86.7	71.7	86.7	75.0
Set 3	66.7	56.7	85.0	96.7	85.0	100.0
Mean	**68.3**	**60.0**	**82.2**	**88.3**	**88.9**	**91.7**
Quadratic						
Set 1	61.7	75.0	70.0	95.0	68.3	100.0
Set 2	76.7	38.3	73.3	76.7	66.7	81.7
Set 3	65.0	73.3	61.7	93.3	60.0	100.0
Mean	**67.8**	**62.2**	**68.3**	**88.3**	**65.0**	**93.9**
Mahalanobis						
Set 1	66.7	45.0	96.7	80.0	76.7	96.7
Set 2	86.7	30.0	93.3	46.7	86.7	61.7
Set 3	78.3	55.0	90.0	81.7	81.7	96.7
Mean	**77.2**	**43.3**	**93.3**	**69.4**	**81.7**	**85.0**

Appendix 3

Two class classification of wheat kernels by various statistical classifiers (Case 1: 300 healthy and 900 all infected kernels)

Set	Linear %	Quadratic %	Mahalanobis %
	Healthy		
Set 1	83.3	76.7	71.7
Set 2	81.7	71.7	75.0
Set 3	83.3	73.3	68.3
Mean	**82.8**	**73.9**	**71.7**
	A. niger		
Set 1	88.3	90.0	91.7
Set 2	91.7	91.7	93.3
Set 3	88.3	88.3	91.7
Average	**89.4**	**90.0**	**92.2**
	A. glaucus		
Set 1	91.7	91.7	91.7
Set 2	90.0	95.0	98.3
Set 3	91.7	86.7	86.7
Average	**91.1**	**91.1**	**92.2**
	Penicillium		
Set 1	88.3	95.0	96.7
Set 2	93.3	98.3	100.0
Set 3	96.7	98.3	100.0
Average	**92.8**	**97.2**	**98.9**

Appendix 4

Two class classification of wheat kernels by various statistical classifiers (Case 2: 300 healthy and 300 mixed infected kernels equal for each species).

	Healthy %	Fungal infected kernels %
Linear		
set1	85.0	80.0
set2	85.0	96.6
set3	90.0	81.6
Mean	**86.7**	**86.1**
Quadratic		
set1	80.0	83.3
set2	73.3	95.0
set3	75.0	81.6
Mean	**76.1**	**86.6**
Mahalanobis		
set1	88.3	75.0
set2	75.0	95.0
set3	71.6	83.3
Mean	**78.3**	**84.4**

Appendix 5

Four class classification of wheat kernels by linear statistical classifier

	Healthy (%)	*A. niger* (%)	*A. glaucus* (%)	*Penicillium* (%)
Healthy				
Set 1	71.7	1.7	13.3	13.3
Set 2	75.0	6.7	8.3	10.0
Set 3	76.7	6.7	8.3	8.3
Mean	**74.4**	**5.0**	**10.0**	**10.6**
A. niger				
Set 1	10.0	58.3	25.0	6.7
Set 2	3.3	51.7	35.0	10.0
Set 3	10.0	61.7	21.7	6.7
Mean	**7.8**	**57.2**	**27.2**	**7.8**
A. glaucus				
Set 1	3.3	36.7	53.3	6.7
Set 2	6.7	20.0	68.3	5.0
Set 3	6.7	21.7	58.3	10.0
Mean	**5.6**	**26.1**	**60.0**	**7.2**

(Continued)

(Continued)

	Healthy (%)	*A. niger* (%)	*A. glaucus* (%)	*Penicillium* (%)
Penicillium				
Set 1	6.7	10.0	15.0	68.3
Set 2	0.0	5.0	0.0	95.0
Set 3	0.0	5.0	1.7	93.3
Mean	**2.2**	**6.7**	**5.6**	**85.6**

Appendix 6

Four class classification of wheat kernels by quadratic statistical classifier

	Healthy (%)	***A. niger*** (%)	***A. glaucus*** (%)	***Penicillium*** (%)
Healthy				
Set 1	70.0	11.7	10.0	8.3
Set 2	70.0	18.3	6.7	5.0
Set 3	68.3	16.7	6.7	8.3
Mean	**69.4**	**15.6**	**7.8**	**7.2**
A. niger				
Set 1	6.7	53.3	15.0	25.0
Set 2	6.7	51.7	16.7	25.0
Set 3	6.7	50.0	31.7	11.7
Mean	**6.7**	**51.7**	**21.1**	**20.6**
A. glaucus				
Set 1	3.3	48.3	33.3	15.0
Set 2	6.7	10.0	58.3	25.0
Set 3	6.7	8.3	60.0	25.0
Mean	**5.6**	**22.2**	**50.6**	**21.7**

(Continued)

(Continued)

	Healthy (%)	*A. niger* (%)	*A. glaucus* (%)	*Penicillium* (%)
Penicillium				
Set 1	3.3	15.0	13.3	68.3
Set 2	0.0	5.0	0.0	95.0
Set 3	0.0	5.0	0.0	95.0
Mean	**1.1**	**8.3**	**4.4**	**86.1**

Appendix 7

Four class classification of wheat kernels by Mahalanobis statistical classifier

	Healthy (%)	*A. niger* (%)	*A. glaucus* (%)	*Penicillium* (%)
Healthy				
Set 1	71.7	16.7	10.0	1.7
Set 2	78.3	16.7	5.0	0.0
Set 3	75.0	20.0	5.0	0.0
Mean	**75.0**	**17.8**	**6.7**	**0.6**
A. niger				
Set 1	6.7	76.7	13.3	3.3
Set 2	11.7	68.3	13.3	6.7
Set 3	10.0	60.0	26.7	3.3
Mean	**9.4**	**68.3**	**17.8**	**4.4**
A. glaucus				
Set 1	3.3	61.7	30.0	5.0
Set 2	6.7	31.7	53.3	8.3
Set 3	6.7	8.3	60.0	25.0
Mean	**5.6**	**33.9**	**47.8**	**12.8**

(Continued)

(Continued)

	Healthy (%)	***A. niger*** (%)	***A. glaucus*** (%)	***Penicillium*** (%)
Penicillium				
Set 1	8.3	33.3	13.3	45.0
Set 2	1.7	20.0	0.0	80.0
Set 3	6.7	16.7	0.0	76.7
Mean	**5.6**	**23.3**	**4.4**	**67.2**

Appendix 8

Pair-wise classification of healthy and fungal infected wheat kernels by BPNN classifiers

	Healthy Vs *A. niger*		Healthy Vs. *A. glaucus*		Healthy Vs. *Penicillium*	
	Healthy (%)	*A. niger* (%)	Healthy (%)	*A. glaucus* (%)	Healthy (%)	*Penicillium* (%)
Training						
Set 1	91.9	79.5	92.4	84.3	85.7	93.3
Set 2	90.8	89.5	90.0	92.4	95.7	97.1
Set 3	87.6	91.4	81.0	91.9	86.7	93.3
Mean	**90.0**	**86.8**	**87.8**	**89.5**	**89.4**	**94.6**
Testing						
Set 1	80.0	81.7	83.3	83.3	85.0	90.0
Set 2	95.0	88.3	70.0	75.0	93.3	86.7
Set 3	75.0	70.0	93.3	93.3	86.7	90
Mean	**83.3**	**80.0**	**82.2**	**83.9**	**88.3**	**88.9**
Validation						
Set 1	93.3	86.7	100.0	80.0	90.0	90.0
Set 2	86.7	90.0	86.7	86.7	90.0	83.3
Set 3	90.0	86.7	83.3	93.3	93.3	93.3
Mean	**90.0**	**87.8**	**90.0**	**86.7**	**91.1**	**88.9**

Appendix 9

Pair-wise classification of fungal infected wheat kernels by BPNN classifiers

	A. niger Vs. *A. glaucus*		*A. niger* Vs. *Penicillium*		*A. glaucus* Vs. *Penicillium*	
	A. niger (%)	*A. glaucus* (%)	*A. niger* (%)	*Penicillium* (%)	*A. glaucus* (%)	*Penicillium* (%)
Training						
Set 1	72.4	47.6	79.5	91.0	82.9	92.9
Set 2	69.5	67.6	86.7	85.7	90.5	88.1
Set 3	69.5	71.4	91.0	83.8	91.9	85.2
Mean	**70.5**	**62.2**	**85.7**	**86.8**	**88.4**	**88.7**
Testing						
Set 1	71.7	56.7	78.3	83.3	80.0	90.0
Set 2	61.7	48.3	85.0	83.3	86.7	85.0
Set 3	71.7	71.7	80.0	81.7	83.3	81.7
Mean	**68.3**	**58.9**	**81.1**	**82.8**	**83.3**	**85.6**

(Continued)

(Continued)

	A. niger Vs. *A. glaucus*		*A. niger* Vs. *Penicillium*		*A. glaucus* Vs. *Penicillium*	
	A. niger	***A. glaucus***	***A. niger***	***Penicillium***	***A. glaucus***	***Penicillium***
	(%)	**(%)**	**(%)**	**(%)**	**(%)**	**(%)**
Validation						
Set 1	73.3	56.7	86.7	76.7	86.7	83.3
Set 2	56.7	53.3	90.0	80.0	86.7	96.7
Set 3	100.0	80.0	90.0	83.3	86.7	96.7
Mean	**76.7**	**63.3**	**88.9**	**80.0**	**86.7**	**92.2**

Appendix 10

Two class classification of healthy and fungal infected wheat kernels by BPNN classifiers (Case 1: 300 healthy and 900 all infected kernels)

	Healthy (%)	*A. niger* (%)	*A. glaucus* (%)	*Penicillium* (%)
Training				
Set 1	70.0	93.3	95.7	97.6
Set 2	63.8	91.4	95.7	92.4
Set 3	54.3	96.7	96.7	97.6
Mean	**62.7**	**93.8**	**96.0**	**95.9**
Testing				
Set 1	65.0	100.0	93.3	98.3
Set 2	58.3	100.0	93.3	95.0
Set 3	50.0	86.7	95.0	93.3
Mean	**57.8**	**95.6**	**93.9**	**95.6**
Validation				
Set 1	70.0	93.3	90.0	96.7
Set 2	66.7	90.0	90.0	96.7
Set 3	43.3	93.3	96.7	100.0
Mean	**60.0**	**92.2**	**92.2**	**97.8**

Appendix 11

Two class classification of wheat kernels by BPNN classifiers (Case 2: 300 healthy and 300 mixed infected kernels equal for each species).

	Healthy %	Fungal Infected kernels %
Training		
Set 1	81.4	89.0
Set 2	89.5	81.9
Set 3	91.4	78.6
Mean	**87.5**	**83.2**
Test		
Set 1	76.7	80.0
Set 2	81.7	90.0
Set 3	83.3	76.7
Mean	**80.6**	**82.2**
Validation		
Set 1	86.7	83.3
Set 2	96.7	86.7
Set 3	93.3	83.3
Mean	**92.2**	**84.4**

Appendix 12

Four class classification of healthy and fungal infected wheat kernels by BPNN classifiers

	Healthy (%)	*A. niger* (%)	*A. glaucus* (%)	*Penicillium* (%)
Training				
Set 1	63.3	12.9	30.0	82.4
Set 2	62.4	22.4	49.0	93.3
Set 3	62.4	26.7	55.2	98.1
Mean	**62.7**	**20.6**	**44.8**	**91.3**
Testing				
Set 1	55.0	11.7	33.3	65.0
Set 2	55.0	18.3	40.0	96.7
Set 3	51.7	23.3	56.7	91.7
Mean	**53.9**	**17.8**	**43.3**	**84.4**
Validation				
Set 1	60.0	10.0	50.0	73.3
Set 2	66.7	13.3	40.0	96.7
Set 3	50.0	13.3	63.3	96.7
Mean	**58.9**	**12.2**	**51.1**	**88.9**